

**NASA
Technical
Memorandum**

NASA TM-86591

**CELESTIAL TARGET OBSERVABILITY FOR
ASTRO SPACELAB MISSIONS**

By Larry D. Mullins

Systems Analysis and Integration Laboratory
Science and Engineering Directorate

March 1987

(NASA-TM-86591) CELESTIAL TARGET
OBSERVABILITY FOR ASTRO SPACELAB MISSIONS
(NASA) 58 p Avail: NTIS EC A04/MF A01
CSCI 22A

N87-22696

Unclas
G3/12 0074267



National Aeronautics and
Space Administration

George C. Marshall Space Flight Center

TABLE OF CONTENTS

	Page
I. INTRODUCTION	1
II. OVERVIEW	1
III. CALCULATING BASIC OBSERVABILITY OF A CELESTIAL TARGET	11
IV. SHIFT IN OBSERVABILITY WITH LAUNCH DELAY	21
V. SHIFT IN OBSERVABILITY WITH MISSION ELAPSED TIME	31
VI. SUN AND MOON INTERFERENCE.....	35
APPENDIX A - DERIVATION OF BETA ANGLE, ARGUMENT-OF-LATITUDE OF CULMINATION, AND ORBITAL ELEVATION ANGLE.....	43
APPENDIX B - CALCULATING THE RIGHT ASCENSION OF THE ASCENDING NODE OF THE ORBIT PLANE	49

PRECEDING PAGE BLANK NOT FILMED

LIST OF ILLUSTRATIONS

Figure	Title	Page
1A.	Illustration of shift in target acq/loss times with passage of time and as a function of target location.....	2
1B.	Illustration of shift in target acq/loss times with passage of time and as a function of target location.....	3
1C.	Illustration of shift in target acq/loss times with passage of time and as a function of target location.....	4
1D.	Illustration of shift in target acq/loss times with passage of time and as a function of target location.....	5
2A.	Illustration of shift in target acq/loss times with launch delay and as a function of target location.....	6
2B.	Illustration of shift in target acq/loss times with launch delay and as a function of target location.....	7
2C.	Illustration of shift in target acq/loss times with launch delay and as a function of target location.....	8
2D.	Illustration of shift in target acq/loss times with launch delay and as a function of target location.....	9
3.	Illustration of the β -angle and argument-of-latitude of culmination of a star.....	12
4.	Target beta angle as a function of target location and orbit plane orientation.....	15
5.	Target observation time as a function of beta angle (orbital elevation angle constraint as a parameter)	16
6.	Target observation time (orbit period fraction) as a function of orbital elevation angle constraint (target beta as a parameter)	18
7.	Argument of latitude of target culmination as a function of target declination (delta between target right ascension and orbit plane ascending node right ascension as parameter).....	19
8.	Argument of latitude of target culmination as a function of the difference between right ascension of target and right ascension of ascending node of orbit plane (target declination as parameter)	20
9A.	Celestial target acq/loss times relative to orbit ascending node for varying target declinations	22
9B.	Celestial target acq/loss times relative to orbit ascending node for varying target declinations	23

LIST OF ILLUSTRATIONS (Concluded)

Figure	Title	Page
10.	Effects of launch delay and nodal regression on angular difference between right ascension of target and right ascension of ascending node of orbit plane	24
11.	Effect of launch delay on target and orbit plane ascending node right ascension difference angle for various assumed initial values ...	25
12.	Regions on the celestial sphere where target acq/loss shift times change from negative to positive with a delay in launch time.....	28
13.	Location on the celestial sphere of regions defined in Figure 12.....	29
14.	Illustration of acq/loss shift of targets on either side of the orbit pole with launch delay	30
15.	Effect of MET on target and orbit plane ascendign node right ascension difference angle - various assumed initial values.....	32
16.	The rate of change of the culmination position in the orbit plane for targets of varying declination and various positions with respect to the orbital plane ($\alpha-\Omega$)	34
17.	Illustrationof Sun in ecliptic plane and angle ϕ of star to be observed out of ecliptic plane	36
18.	The solar position and the region of solar avoidance over an annual cycle	41
19.	The lunar position with the day-time and night-time lunar avoidance regions shown for a one-month time period	42
A-1.	Illustration of minimum OEA for a given atmospheric constraint.....	48
B-1.	Illustration of the ascending node of the orbit plane relative to the meridian of Greenwich, England, and to the vernal equinox	52
B-2.	Right ascension of the ascending node of the orbit plane as a function of launch date and launch time for ASTRO orbits ($i = 28.^{\circ}5$, Alt = 350 km).....	53

TECHNICAL MEMORANDUM

CELESTIAL TARGET OBSERVABILITY FOR ASTRO SPACELAB MISSIONS

I. INTRODUCTION

When planning an observing schedule for conducting an astronomical mission from orbit, one of the first pieces of data required is the observing time available for targets at various locations on the celestial sphere. Instead of just putting a target "in the hopper" and letting it "flow through the mission planning cycle," it would be useful to know in advance what to expect in the way of observation time for that target based on its position relative to the orbit plane. This would be especially pertinent if one were trying to substitute a new target during real time replanning. Information of this nature would allow the Principal Investigator (PI) or the mission planner to determine the region of the celestial sphere from which it would be most desirable to select targets and those regions to avoid selecting targets from in order to obtain a more optimum observing schedule for a given orbit (or mission). It is precisely this question which will be addressed in this report.

II. OVERVIEW

Observational data can be generated by uniformly distributing targets on a meridian plane in declination from -90° to $+90^\circ$ and varying the position of the orbit plane with respect to those targets. In this report, this variation of position will be measured by the difference between the right ascension of the target, α , and the right ascension of the ascending node of the orbit plane, Ω ; i.e., by the quantity $(\alpha - \Omega)$. The acquisition and loss times of these targets can be calculated and presented in the form of graphs. These, for a generic orbit and a generic set of targets, are presented in Figures 1A through 1D and 2A through 2D. The orbit chosen has an inclination of $28.^\circ 5$, right ascension of the ascending node of 0° and an orbital period of about 1 hr 31 min (ALT \approx 350 km). (These orbital parameters are representative of the ASTRO-1 mission.) The targets in Figure 1A are lying in a plane of $\alpha = 0^\circ$ such that $\alpha - \Omega = 0^\circ$ for that figure. The targets in Figures 1B, 1C, and 1D are at $\alpha = 90^\circ$, 180° , and 270° , respectively. The declinations of the targets range from -90° to $+90^\circ$ on each figure. There are two sets of curves on each figure: one set corresponding to the start of the mission observations at MET = 24 hr, and the second set to the end of the mission at 192 hr MET. This allows one to observe the relative movement of the On/Off times with the passage of time (Mission Elapsed Time). The reference time of these plots is at an ascending node. From these charts one can then see the on and off time relative to an ascending node or relative to a rev start time. The shifting of the target's acq/loss positions (relative to the ascending node) with mission elapsed time reflects the effects of the movement of the orbit plane relative to inertial space (regression of the nodes). It can be seen that the effect is not uniform over all declinations.

Starting with Figure 1A where the targets have the same right ascension as that of the ascending node of the orbit plane ($\alpha - \Omega = 0^\circ$), one sees that the acquisition of the target occurs prior to the ascending node of the orbit and those at

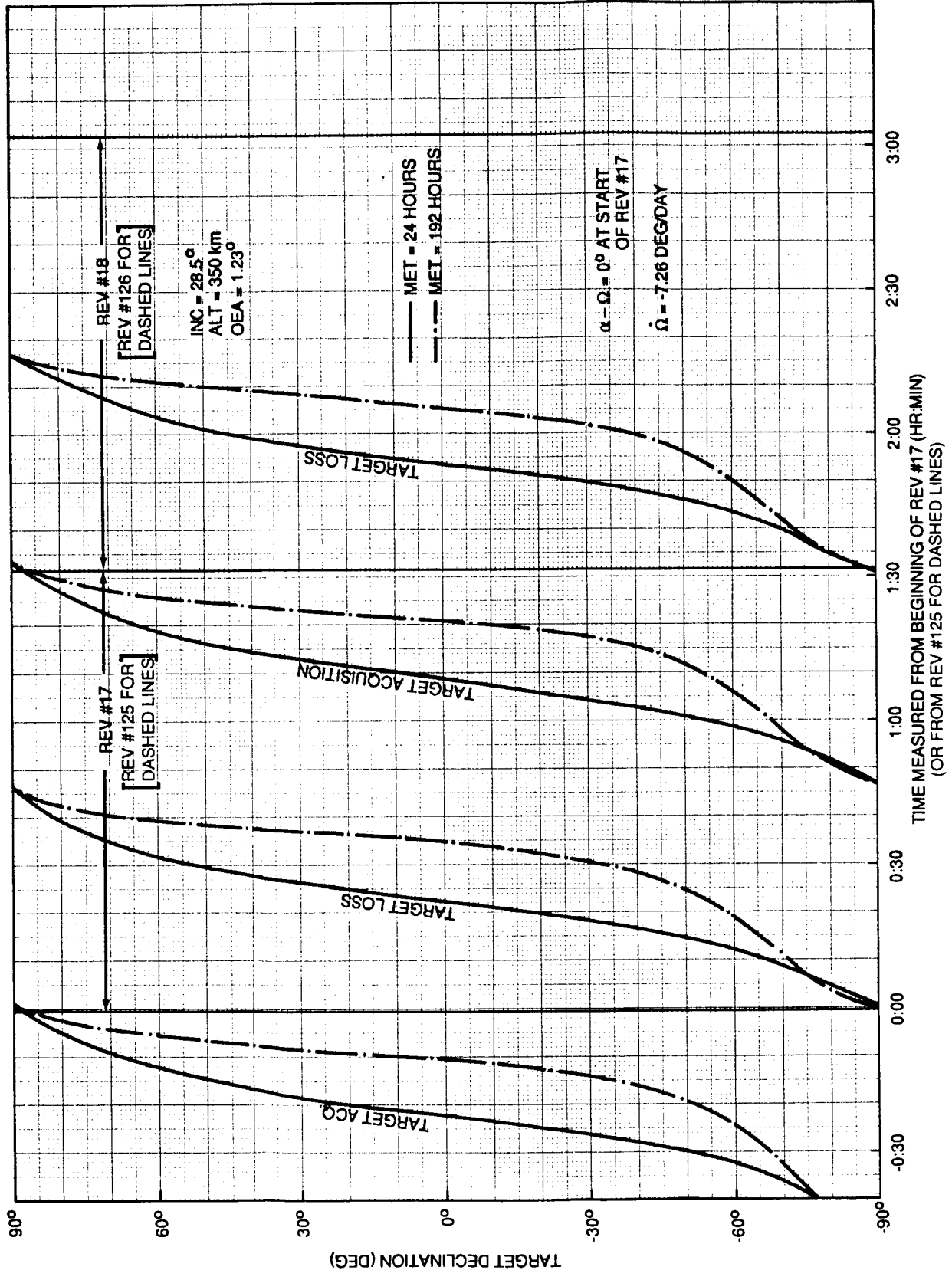


Figure 1A. Illustration of shift in target acq/loss times with passage of time and as a function of target location.

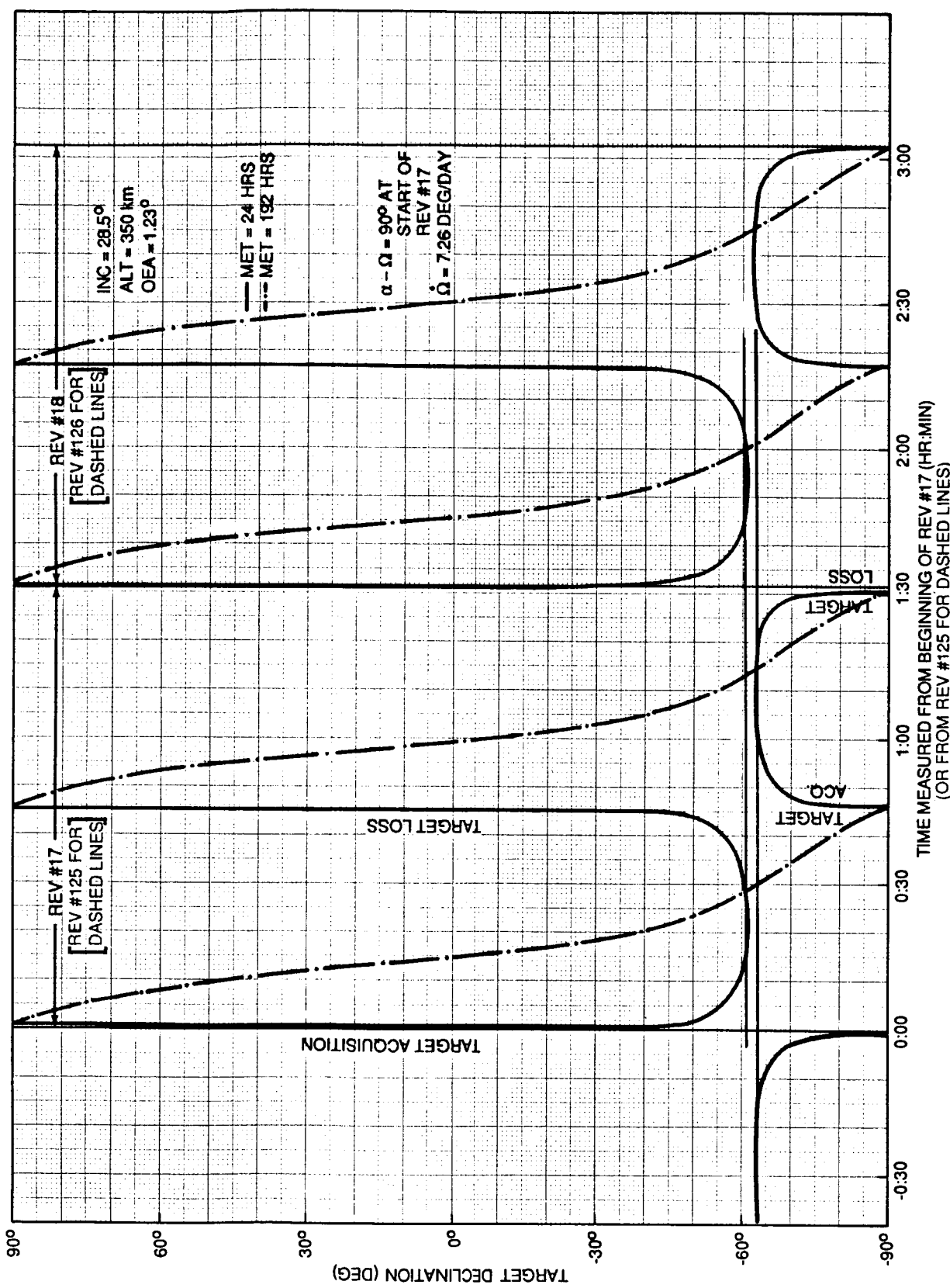


Figure 1B. Illustration of shift in target acq/loss times with passage of time and as a function of target location.

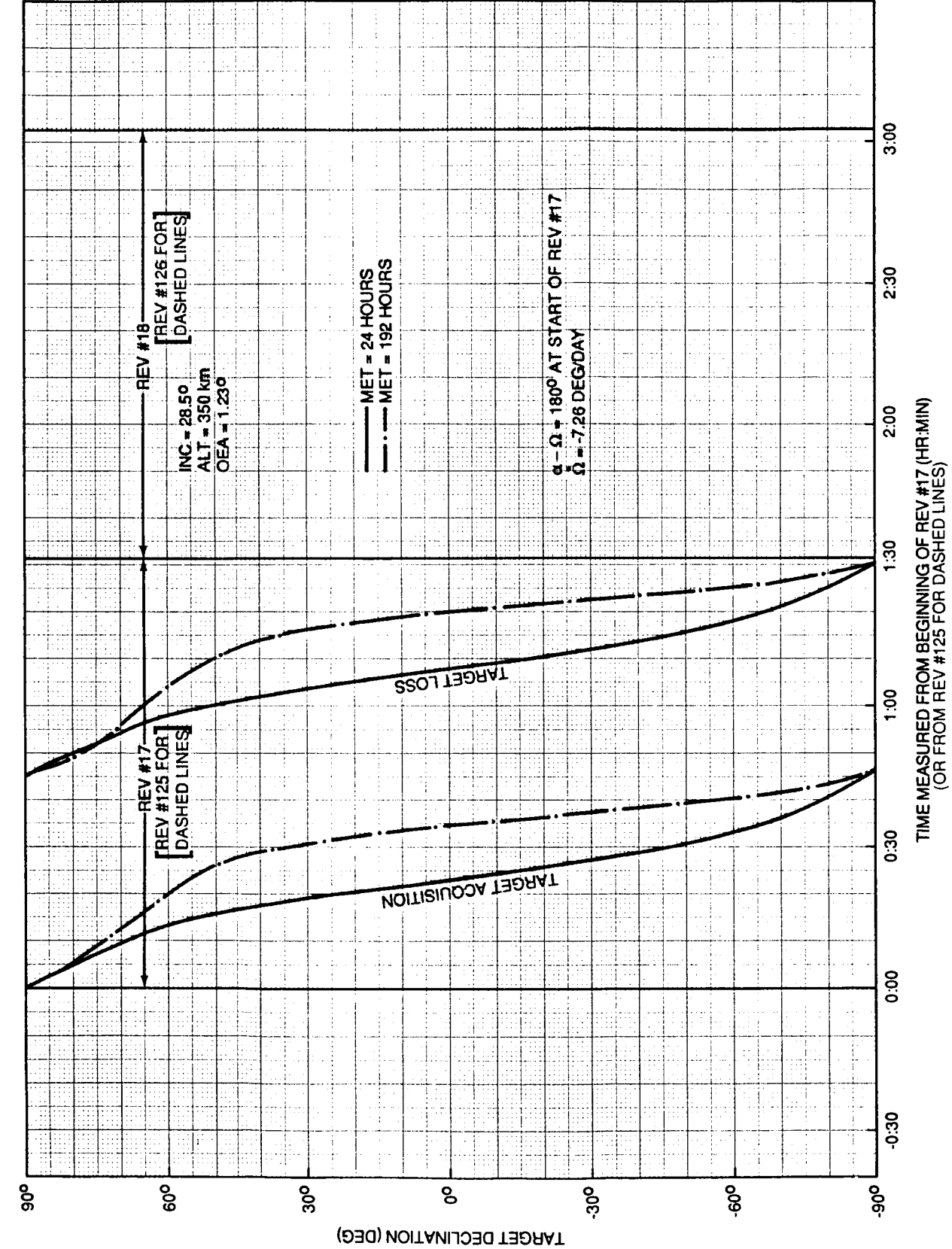


Figure 1C. Illustration of shift in target acq/loss times with passage of time and as a function of target location.

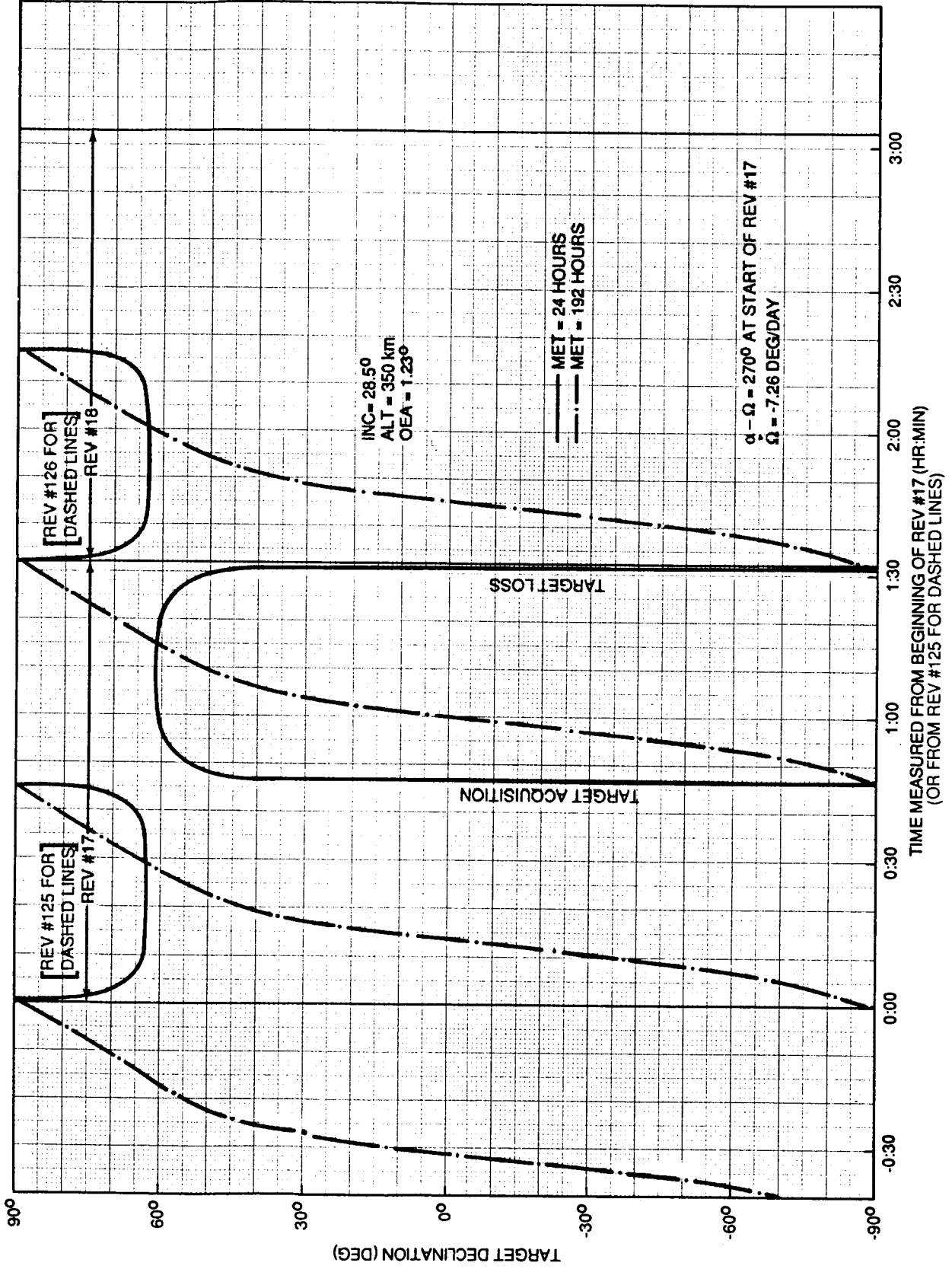


Figure 1D. Illustration of shift in target acq/loss times with passage of time and as a function of target location.

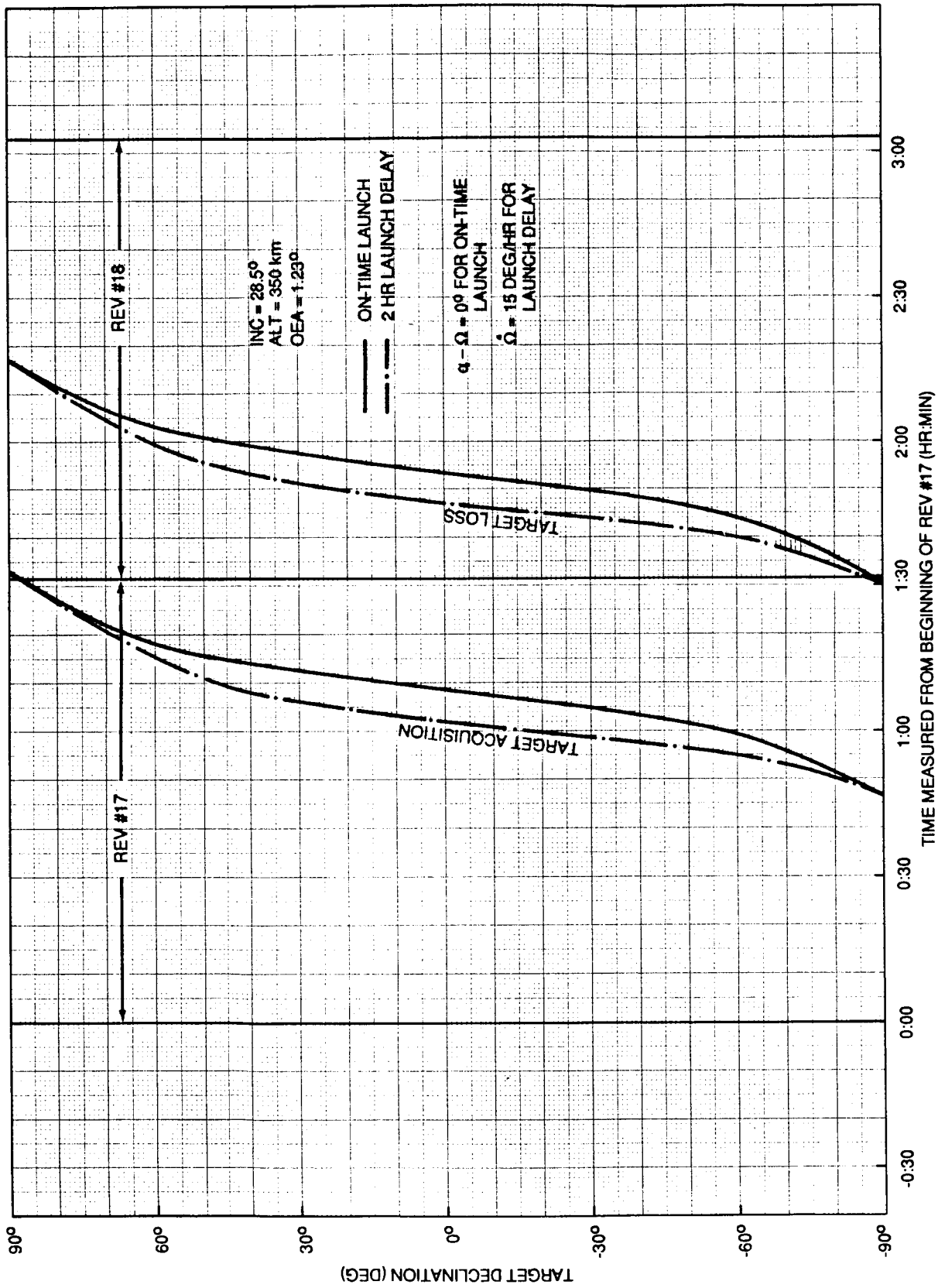


Figure 2A. Illustration of shift in target acq/loss times with launch delay and as a function of target location.

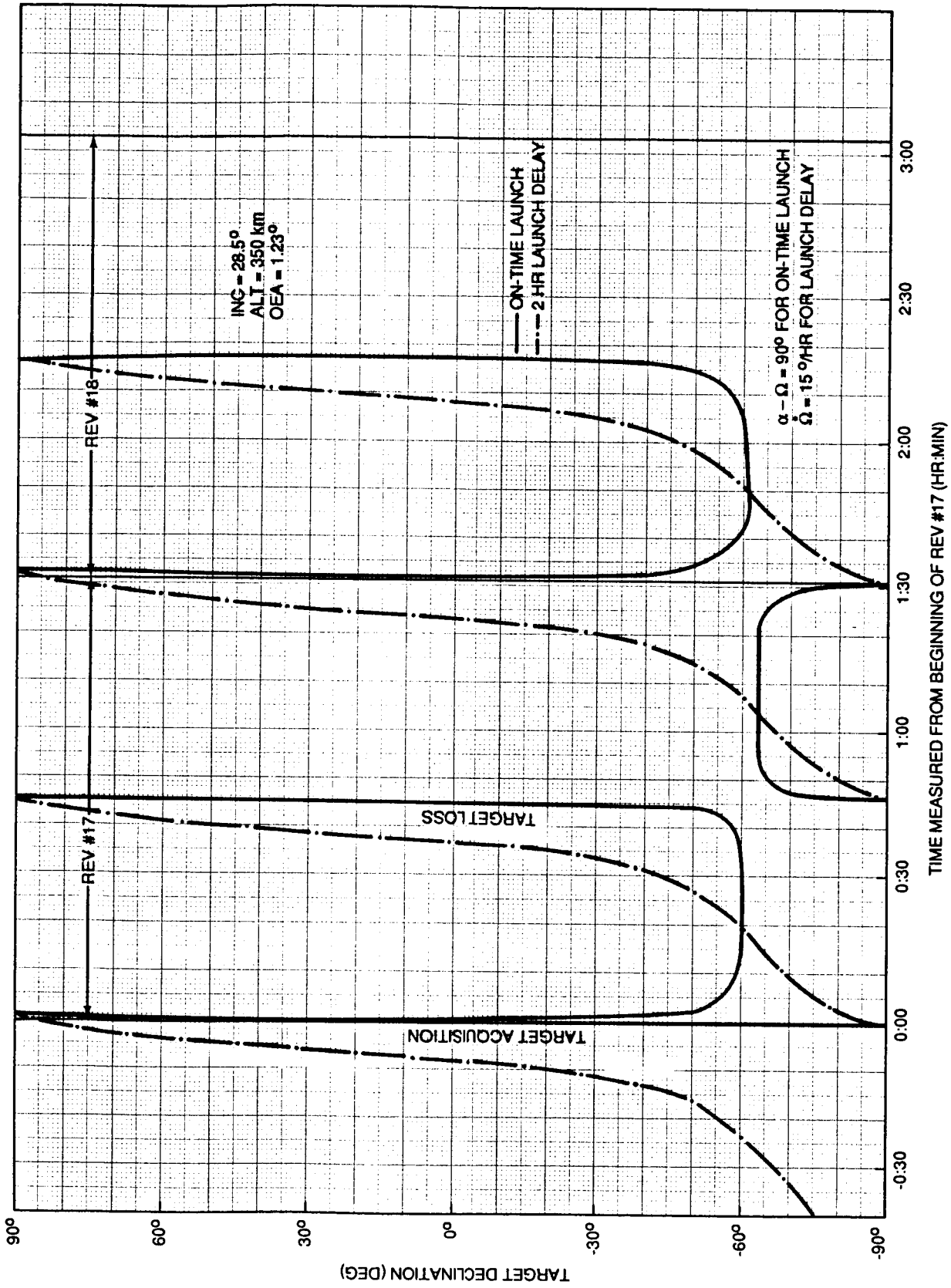


Figure 2B. Illustration of shift in target acq/loss times with launch delay and as a function of target location.

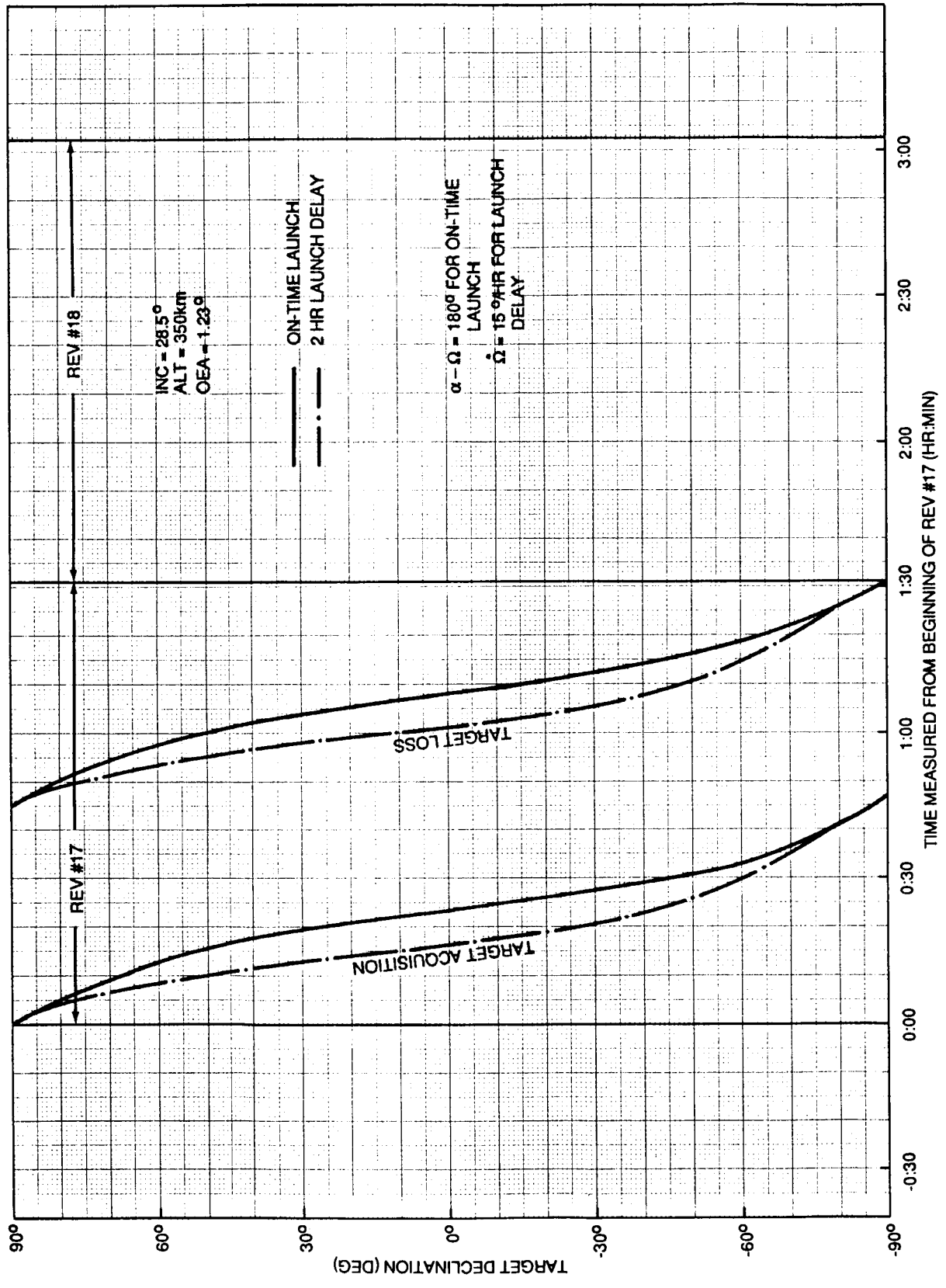


Figure 2C. Illustration of shift in target acq/loss times with launch delay and as a function of target location.

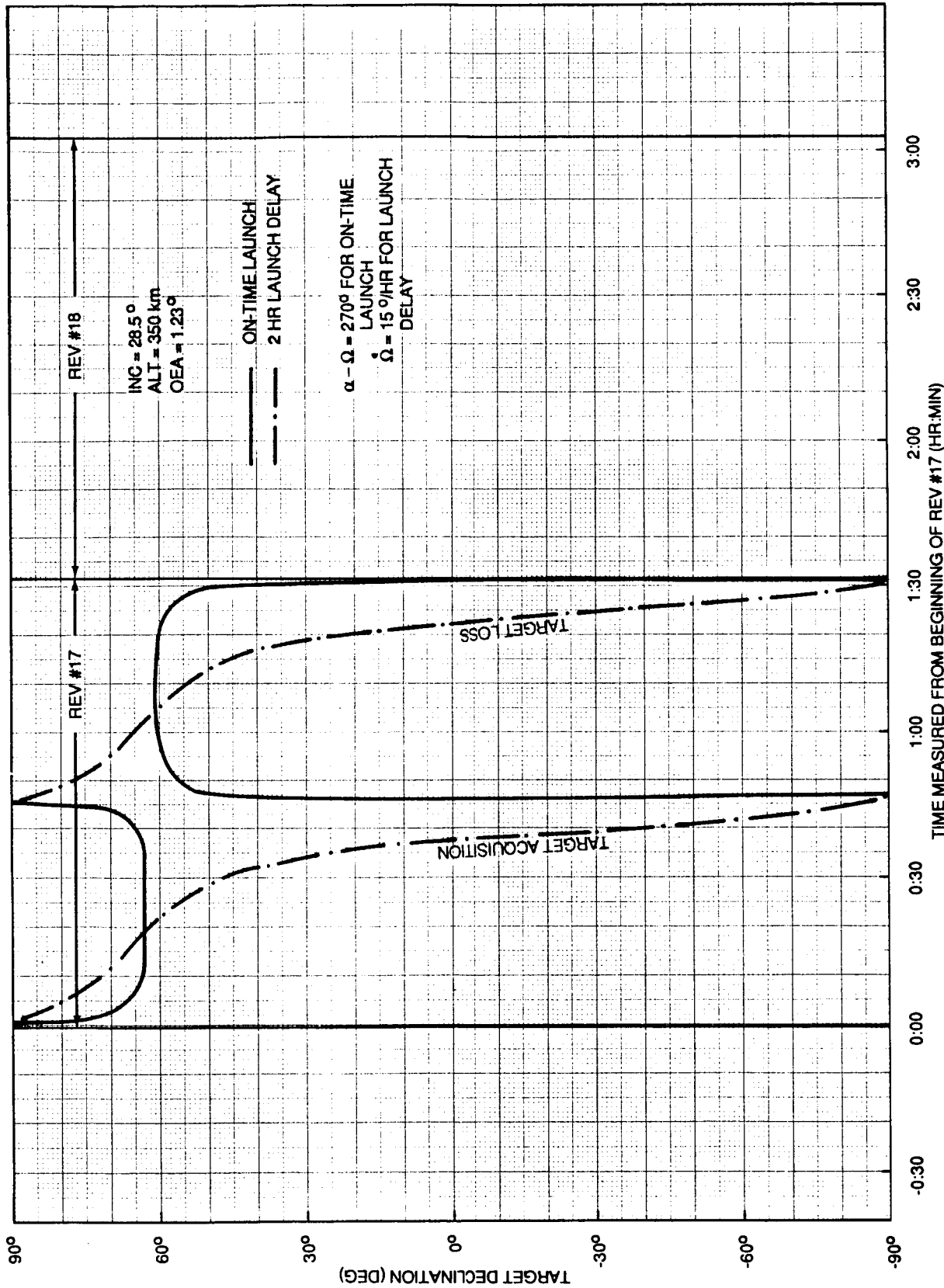


Figure 2D. Illustration of shift in target acq/loss times with launch delay and as a function of target location.

negative declinations are acquired earlier than those at positive declinations. As one shifts to Figure 1B, 1C and 1D where $\alpha-\Omega$ increases to 90° , 180° , and 270° , respectively, one sees that the targets are acquired progressively later in the orbit. At $\alpha-\Omega = 180^\circ$ the situation regarding the relative acquisitions of targets is reversed from that of $\alpha-\Omega = 0^\circ$. Here the targets at positive declination are acquired earlier than those at negative declinations.

One can observe from Figure 1A that, with the exception of targets directly above the Earth's poles, all target acquisition times at the end of the mission are shifted forward in time relative to that target's acquisition time at the start of the mission.

The time shifts for targets at high (absolute) declinations are smaller than those for targets near the equator. The absolute lengths of the observing times do not appear to depend much on the target declination.

Going on to Figure 1B, where $\alpha-\Omega = 90^\circ$, one observes that targets near the equator and at high positive declination exhibit the same general sort of behavior as that observed in Figure 1A. However, as one gets to high negative declinations, one observes some unusual or different behavior. (The same thing can be seen in Figure 1D where $\alpha-\Omega = 270^\circ$ for targets of high positive declination.) In Figure 1B, the target at a -60° declination has a much shorter observing time than the other targets and the targets below -63° declination are shifted backward in the orbit plane with the passage of time rather than forward as has been the case for all other targets so far discussed. This same behavior can be observed in Figure 1D for targets above $+63^\circ$ declination. This phenomenon will be explained in detail later. It will be seen to be due to the fact that the targets are near the orbit poles.

Figures 2A through 2D are presented by the same scheme as that used for the first set of figures, but here the purpose is to show the effect of a launch delay. In Figure 2A one can see that the acq/loss times for a launch delay are shifted backward (earlier) in time relative to the nominal launch. Each hour of launch delay causes the right ascension of the ascending node of the orbit plane to increase by 15° (due to the eastward rotation of the Earth). This is why the acq/loss times occur earlier for launch delays; i.e., the orbit plane, in effect, is rotating into the target (rotating in the same direction as the orbital motion enabling the spacecraft to get to the target at a fixed point sooner).

Note again in Figure 2B the atypical behavior at large negative declinations for $\alpha-\Omega = 90^\circ$ (near the orbit pole) and in Figure 2D at large positive declinations for $\alpha-\Omega = 270^\circ$ (near the other orbit pole). It is also noteworthy that as one approaches the orbit poles, the shift in the acq/loss times of the targets becomes quite large. In this case (2 hr delay), as an example, the target at -50° declination with $\alpha-\Omega = 90^\circ$, the shift is approaching 50 percent of the length of the total observation time which is quite significant for replanning efforts in the event of a launch delay.

Without dwelling at length on all of the little nuances that might be observed from these charts, we summarize some of the major points and then pass on to the analysis:

- All target acq/loss times are shifted forward in the orbit plane (relative to the node), i.e., occur later with the passage of time except those near the orbit poles.

- All target acq/loss times occur earlier with launch delays except those near the orbit poles.
- The magnitude of the shifts due to either the passage of mission time or to launch delays is dependent on the target's position with respect to the orbit plane.
- Although not shown by these figures, it will be shown in the analysis to follow that the length of the observation time is highly dependent on the target's " β -angle" and on the elevation angle above which one is constrained to view the target.

In the following sections, an analytical discussion of these effects will be given which will provide some insight into their behavior.

III. CALCULATING BASIC OBSERVABILITY OF A CELESTIAL TARGET

The amount of time that an astronomical object (e.g., a star) can be observed from a spacecraft in orbit about the Earth depends on the location of that object relative to the orbit plane of the spacecraft and on the constraints placed on the observation; e.g., how far from the Earth's limb it must be at the time of observation. The location of the astronomical object relative to the orbit plane is measured by two angles. The first angle is a measure of how far out of the orbit plane the object is located. This is called its beta (β) angle. The second angle is the angular distance from the ascending node of the orbit plane to the projection of the object's position vector onto the orbit plane. The location of the projection of the object's position vector onto the orbit plane is the culmination point of the object which is the place in the orbit plane where the object attains its minimum zenith angle or maximum elevation angle. The angle measured in the orbit plane from its ascending node to this culmination point is called the argument-of-latitude of culmination of that object, denoted by u_C .

These angles, β and u_C , can be calculated from a knowledge of the orbit plane's orientation with respect to the standard inertial coordinate system (X-axis to the vernal equinox and Z-axis to the North Pole as shown in Fig. 3) and the star's position with respect to this system. The orientation of the orbit plane is measured by its inclination, i , with respect to the equatorial plane and the right ascension of the ascending node, Ω , measured relative to the vernal equinox. The star's coordinates are right ascension, α , and declination, δ . All of these angles are illustrated in Figure 3.

By knowing the unit orbital angular momentum vector (\hat{J}) of the orbit (the orbit pole) and the unit position vector to the star, \hat{R} , one can calculate the β -angle as

$$\hat{R} \cdot \hat{J} = \cos (90-\beta) = \sin \beta \quad . \quad (1)$$

Substituting the appropriate expressions into \hat{R} and \hat{J} gives

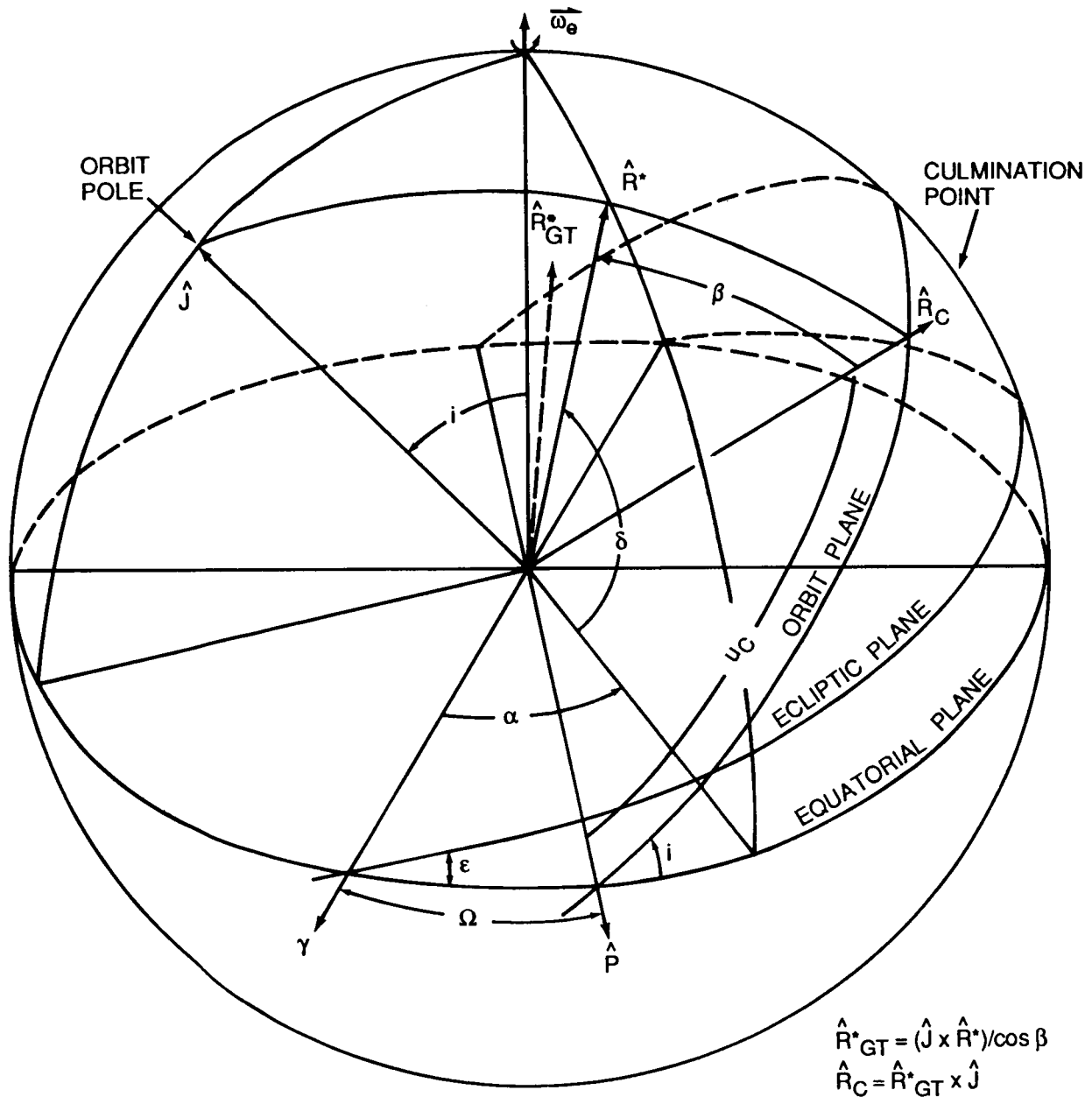


Figure 3. Illustration of the β -angle and argument-of-latitude of culmination of a star.

$$\sin \beta = \cos i \sin \delta - \cos \delta \sin i \sin (\alpha - \Omega) \quad . \quad (2)$$

This is the first of the two angles which measures the location of the object relative to the orbit plane.

By defining unit vectors to the ground terminator of the star, \hat{R}_{GT} , the culmination position of the star, \hat{R}_C , and the ascending node, \hat{P} , as illustrated by Figure 3, one can calculate the second of the two angles, u_C , as,

$$\cos (u_C + 90^\circ) = -\sin u_C = \hat{R}_{GT} \cdot \hat{P} \quad \text{also,} \quad \cos u_C = \hat{R}_C \cdot \hat{P} \quad , \quad (3)$$

which, on substituting in the appropriate expressions for the vectors, gives

$$\tan u_C = \frac{[\sin i \sin \delta + \cos i \cos \delta \sin (\alpha - \Omega)]}{\cos \delta \cos (\alpha - \Omega)} \quad . \quad (4)$$

These equations are derived in detail in Appendix A.

The constraint on observing an object is usually measured by its zenith angle, the angle that the object's position vector makes with respect to the local vertical or else the complement of this angle, the orbital elevation angle (OEA), the angle which the object's position vector makes with respect to the local horizontal plane. If \hat{R}_V is the unit position vector of the orbiting vehicle, then the orbital elevation angle, OEA, of a star with position vector \hat{R} is

$$\hat{R}_V \cdot \hat{R} = \cos (90 - \text{OEA}) = \sin \text{OEA} \quad , \quad (5)$$

from which, with a little manipulation, one can calculate

$$\sin \text{OEA} = \cos \beta \cos (u_C - u) \quad , \quad (6)$$

where u is the current or instantaneous argument of latitude of the vehicle. Equation (6) yields a continuously varying OEA as u is varied by the vehicle traveling around the orbit plane. Conversely, OEA can be viewed as a constraint angle above which one wishes to observe the target star.

One can, with that view, invert equation (6) to calculate the arguments-of-latitude of acquisition and loss (u_A and u_L) of the target star above the given OEA as

$$u_{A,L} = u_C \mp \cos^{-1} \left[\frac{\sin \text{OEA}}{\cos \beta} \right] \quad . \quad (7)$$

The acquisition and loss positions are symmetrically placed on either side of the culmination of the target star.

The length of observation of a target star is given by $u_L - u_A$ divided by the vehicle's rate of travel in the orbit plane (its mean motion, n) and is given by

$$OT = 2 \cos^{-1} \left[\frac{\sin OEA}{\cos \beta} \right] / n \quad , \quad (8)$$

where $n = \sqrt{\mu/a^3}$ (μ is the Earth's gravitational constant and a is the mean semi-major axis of the orbit).

From these basic equations one can deduce practically all information about the possible observation times of objects at various locations relative to the orbit plane. These equations will be analyzed on the following pages.

Before proceeding, it will be beneficial to point out an important behavioral characteristic of the angles β and u_C . Looking at the equations defining them, equations (2) and (4), it is seen that they are dependent on the target star's coordinates α , δ , and the orbit plane's orientation angles i and Ω . The angles α , δ , and i are all constant and Ω changes only slowly with time (on the order of $5^\circ/\text{day}$) so that β and u_C , while not constant, change only very slowly with time. Due to this very slow variation, they can, with little loss of accuracy, be considered constant over one orbit while using equation (7) to compute the acquisition and loss of a target.

A plot of the β -angle of stellar targets with varying declination and parameterized orbit plane placement ($\alpha-\Omega$) for an orbit with fixed inclination, i , is shown in Figure 4. For the orbit plane orientations $\alpha-\Omega = 270^\circ$ and 90° , the corresponding β -angles, as given by equation (2), are $\delta+i$ and $\delta-i$, respectively; thus, in the first instance, where $\delta = 90^\circ-i$ the β -angle becomes 90° and in the second instance where $\delta = i - 90^\circ$ the β -angle becomes -90° . The upper and lower curves in Figure 4 corresponding to $\alpha-\Omega = 270^\circ$ and 90° , respectively, provide an envelope within which all β -angle curves must fall.

The β -angle of a target determines the length of time that the target can be observed as can be seen from equation (8). It also can be observed from equation (8) that the cosine of the observation time for a given target is inversely proportional to the cosine of the β -angle for that target; consequently, when the β -angle of a target gets large its observation time gets small for positive OEAs. In fact, if $\beta > (90^\circ - OEA)$ there is no observation time for that target.

The line of sight to a celestial target for an observer on the surface of the Earth is occulted by the Earth for negative elevation angles. From orbit, however, objects can be observed with negative elevation angles. For negative OEAs, the observation time of a target gets large for large β -angles. In fact, one gets continuous observation of a target if $\beta > 90^\circ - |OEA|$ for negative OEAs.

The observation time for a celestial target as a fraction of the orbital period is shown in Figure 5 as a function of β -angle with OEA parameterized. In summary, if $|\beta| > 90^\circ - |OEA|$ there is no observation time for positive OEA constraint values and

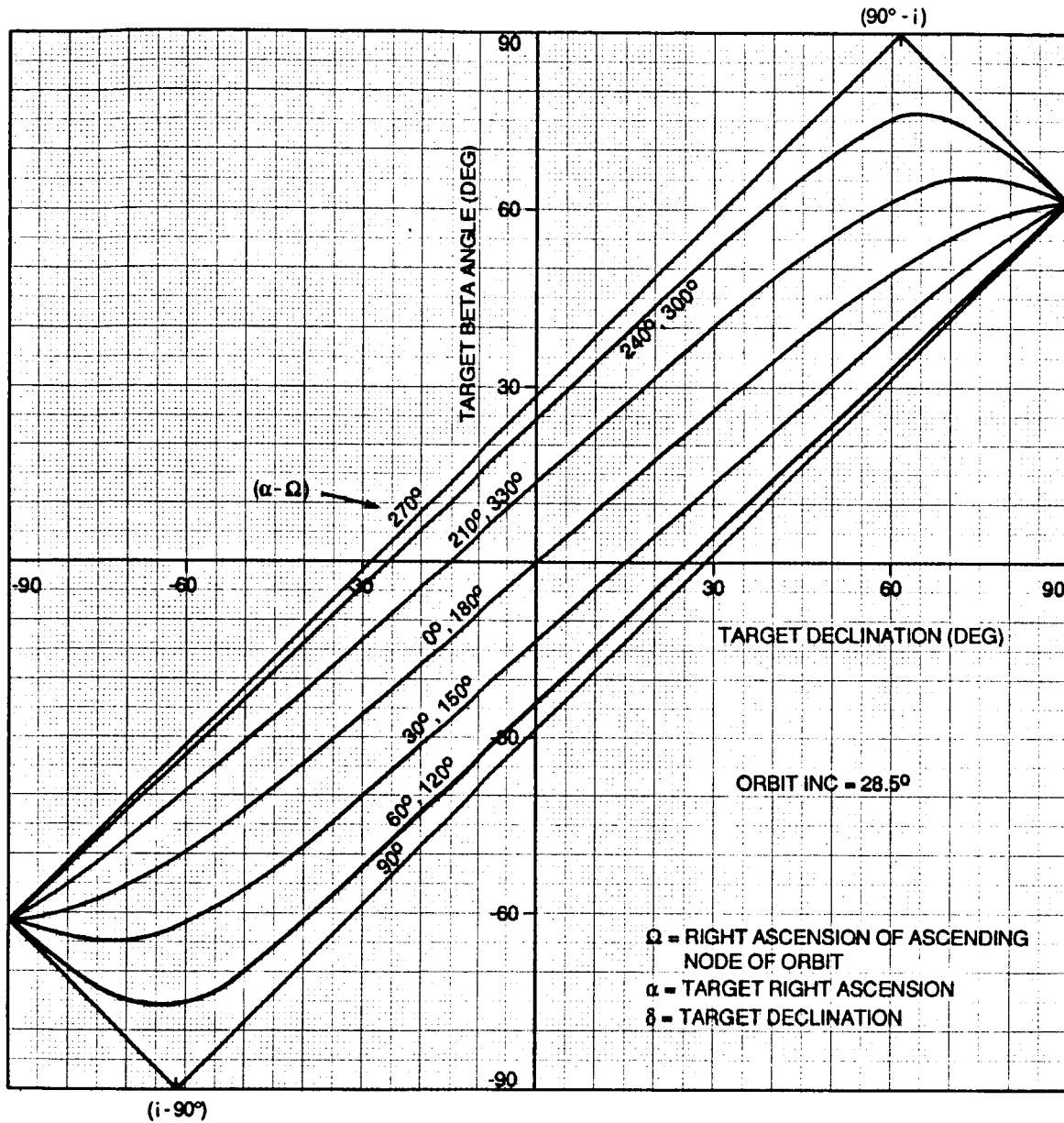


Figure 4. Target beta angle as a function of target location and orbit plane orientation.

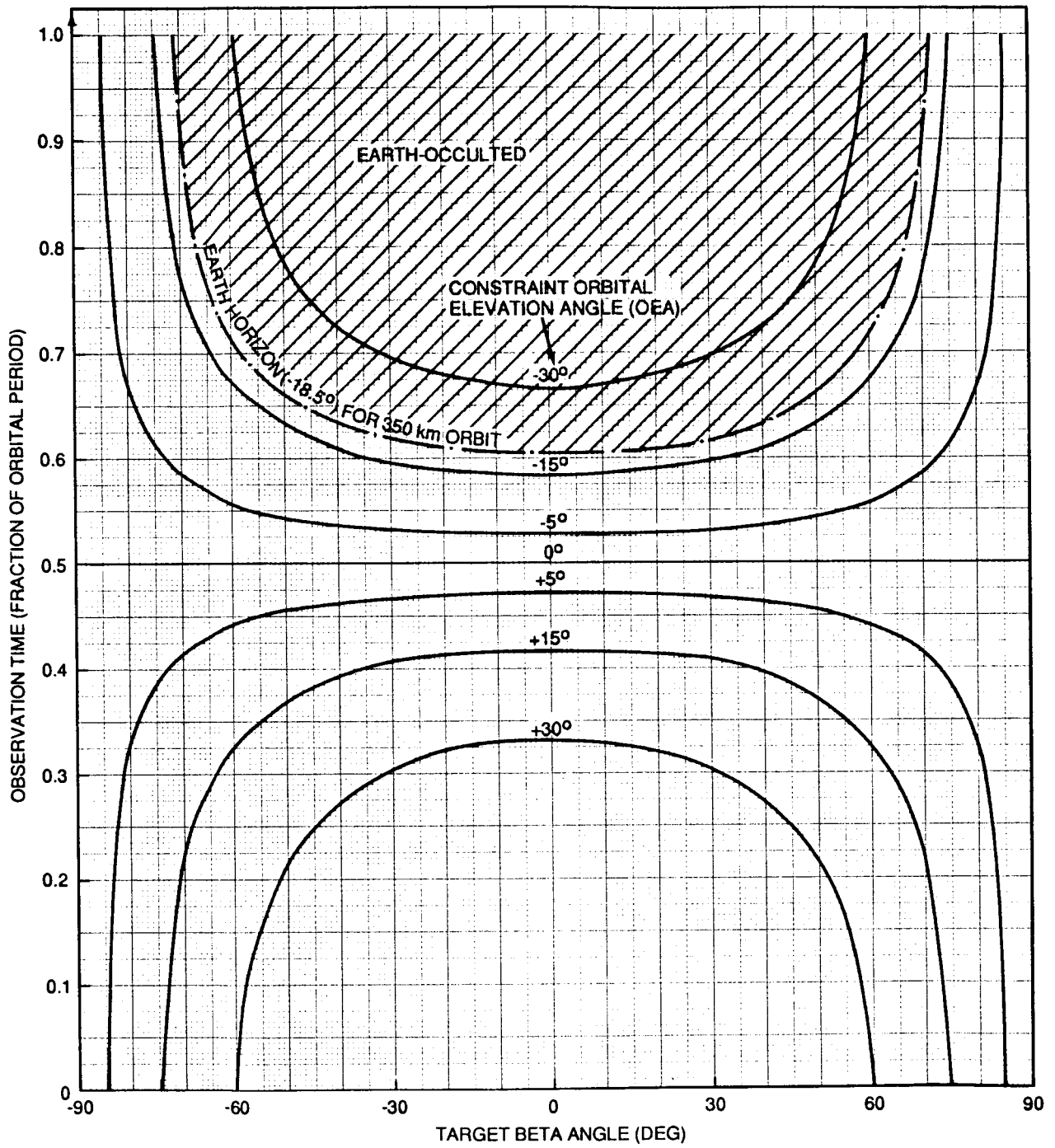


Figure 5. Target observation time as a function of beta angle (orbital elevation angle constraint as a parameter).

continuous observation time for negative OEA constraint values. For a constraint OEA of 0° one can observe the target for exactly 1/2 of the orbit for all β -angles except $\pm 90^\circ$ which are singularities, $\cos^{-1}(0/0)$. These are cases where the target sits always on the horizon of the plane defined by $OEA = 0^\circ$, never rising and never setting.

The amount of observation time per orbit can also be presented as a function of the OEA constraint above which it is desired to view the target with the β -angle of the target parameterized. The plot of the data in this form is shown in Figure 6. Although constraint OEAs are shown to -90° in this plot for completeness, it is not physically possible to observe targets with OEAs below -15° or -20° depending on the altitude of the orbit because of occultation of the target by the Earth.

The location in the orbit plane where a target is visible depends on where the culmination of that target occurs in the orbit plane. The argument-of-latitude of culmination of a target with coordinates (α, δ) in an orbit plane with inclination i and right ascension of the ascending node Ω is given by equation (4). Plots of this angle for targets of varying declination δ are shown in Figure 7 for a fixed orbital inclination i and with the orbit plane orientation with respect to the target $(\alpha-\Omega)$ parameterized. The acquisition and loss of a target is symmetrically placed on either side of culmination and these values depend on the constraint OEA above which it is desired to view the target; for example, for $OEA = 0^\circ$ the acquisition is 90° prior to u_C and the loss is 90° following u_C .

If one knows the orbit plane orientation with respect to a target $(\alpha-\Omega)$ and the target declination, δ , then one can tell quickly from this chart where in the orbit plane that target will be visible; for example, if $\alpha-\Omega = 60^\circ$, a target at 30° declination would have a u_C at about 64° . For a constraint OEA of 0° it would become visible at $u_A = 64^\circ - 90^\circ = -26^\circ = 334^\circ$ and would be lost at $u_L = 64^\circ + 90^\circ = 154^\circ$. Thus, its acq/loss would straddle the ascending node of the orbit, or the acquisition would occur on one orbit and the loss on the following orbit.

This same information is presented in a different form in Figure 8. There the argument-of-latitude of culmination, u_C , is presented as a function $(\alpha-\Omega)$ with declination of the target, δ , parameterized. Both of these figures are for an orbit with an inclination of 28.5° which results from a due east launch from Cape Kennedy.

Either one of these figures (7 or 8) shows how one can get some very large changes in the acquisition and loss time of a target with only a very small change in a target's position with respect to the orbit plane $[(\alpha-\Omega)$ and $\delta]$. As an example of this, consider a target at 60° declination with $(\alpha-\Omega) = 260^\circ$. Figure 8 shows the u_C to be about 210° . If $(\alpha-\Omega)$ is increased to 280° , the u_C dramatically increases to about 340° . This is an increase of 130° in the orbit plane which would correspond to a acq/loss shift in time of about 33 minutes or about 1/3 of an orbit. On the other hand, for a target at a slightly higher declination, say about 65° , for $(\alpha-\Omega) = 260^\circ$ its u_C would be about 140° and if $(\alpha-\Omega)$ was increased to about 280° its u_C would dramatically decrease to about 40° , or a decrease of 100° in the orbit plane. Thus, two targets separated by only 5° in declination would experience extreme and opposite shifts in acq/loss times with only a relatively small change in the orbit plane orientation. The basic reason for this is that one of the targets is higher in declination than the orbit pole and the other is lower. The β -angle for either target, by Figure

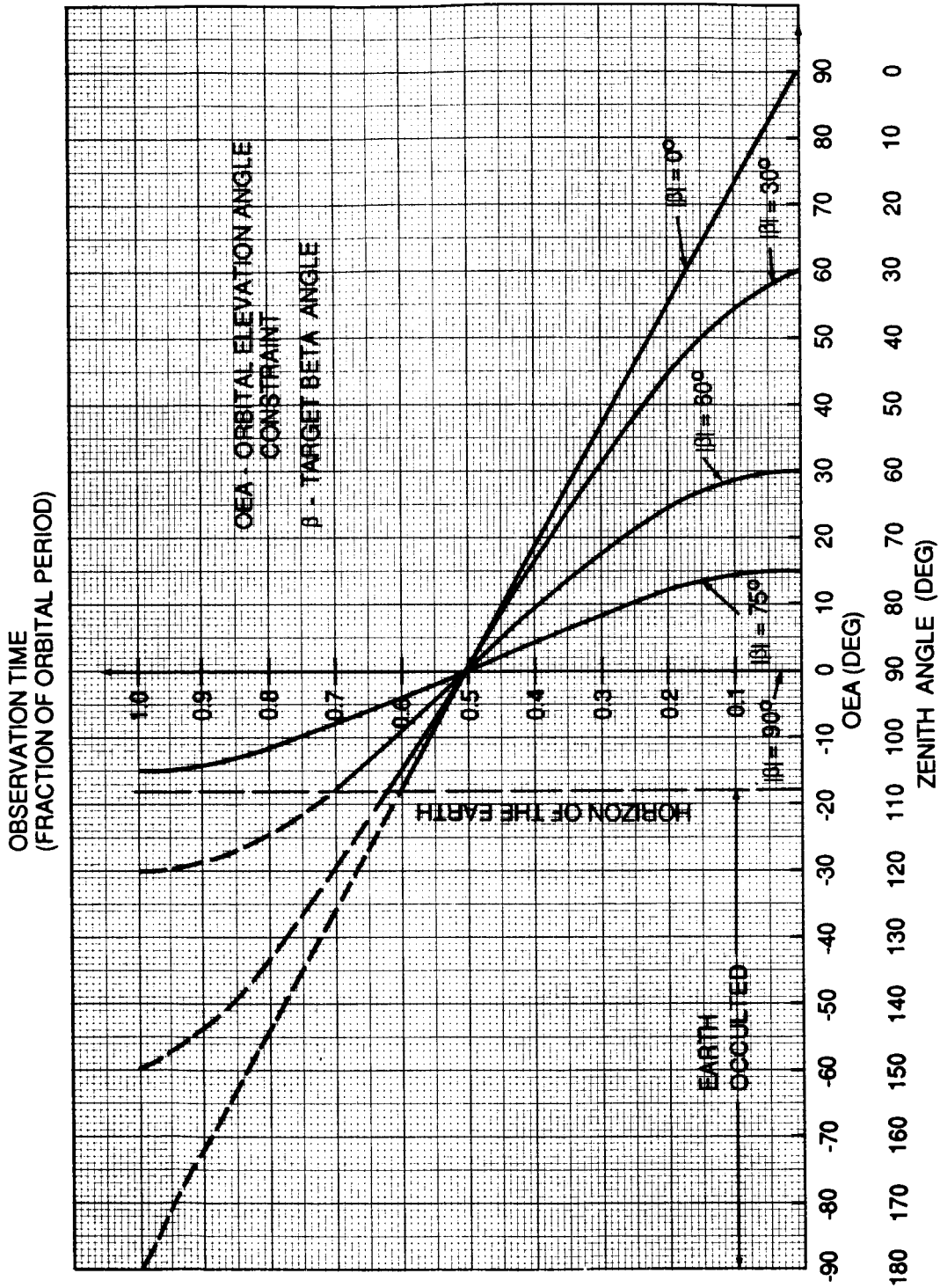


Figure 6. Target observation time (orbit period fraction) as a function of orbital elevation angle constraint (target beta as a parameter).

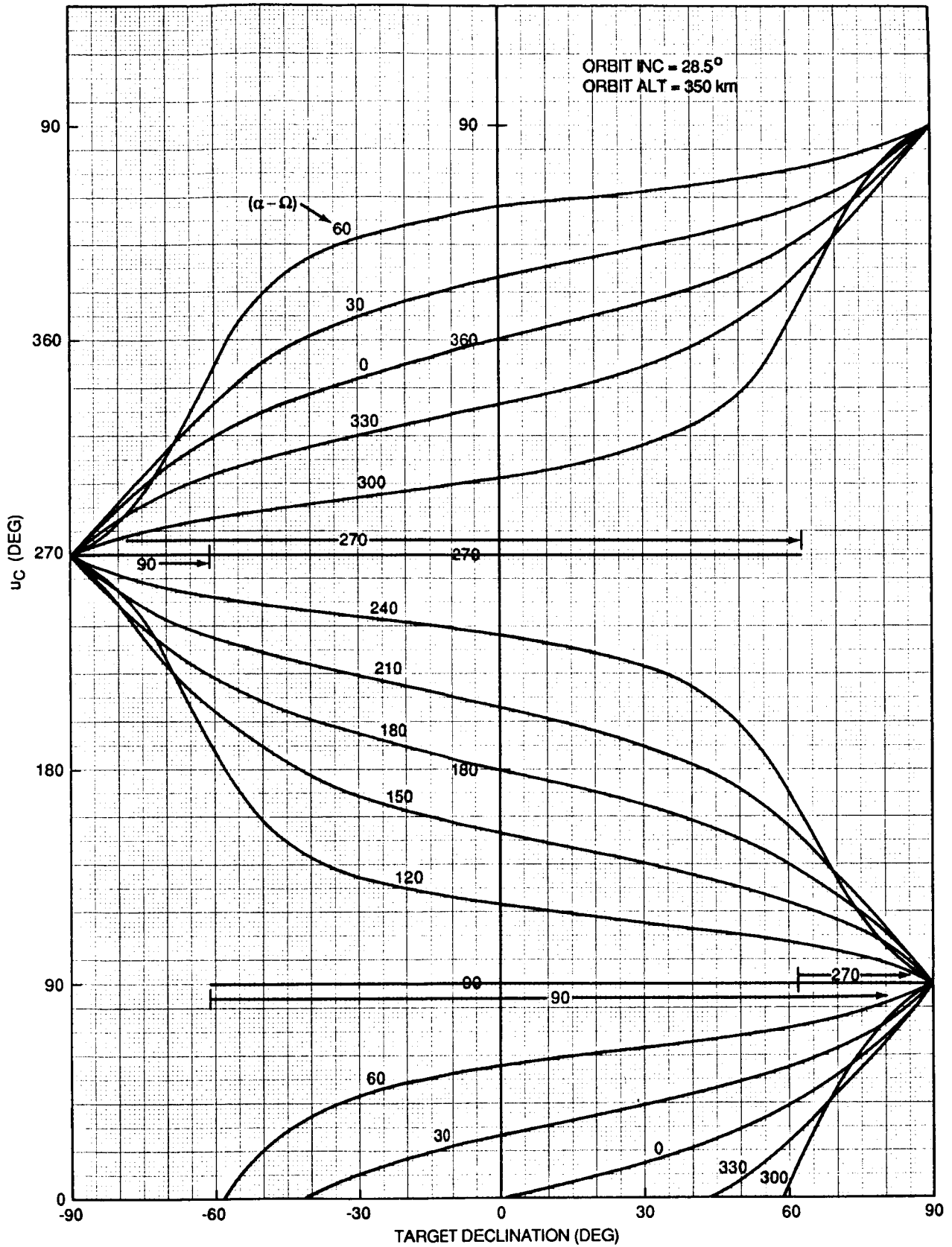


Figure 7. Argument of latitude of target culmination as a function of target declination (delta between target right ascension and orbit plane ascending node right ascension as parameter).

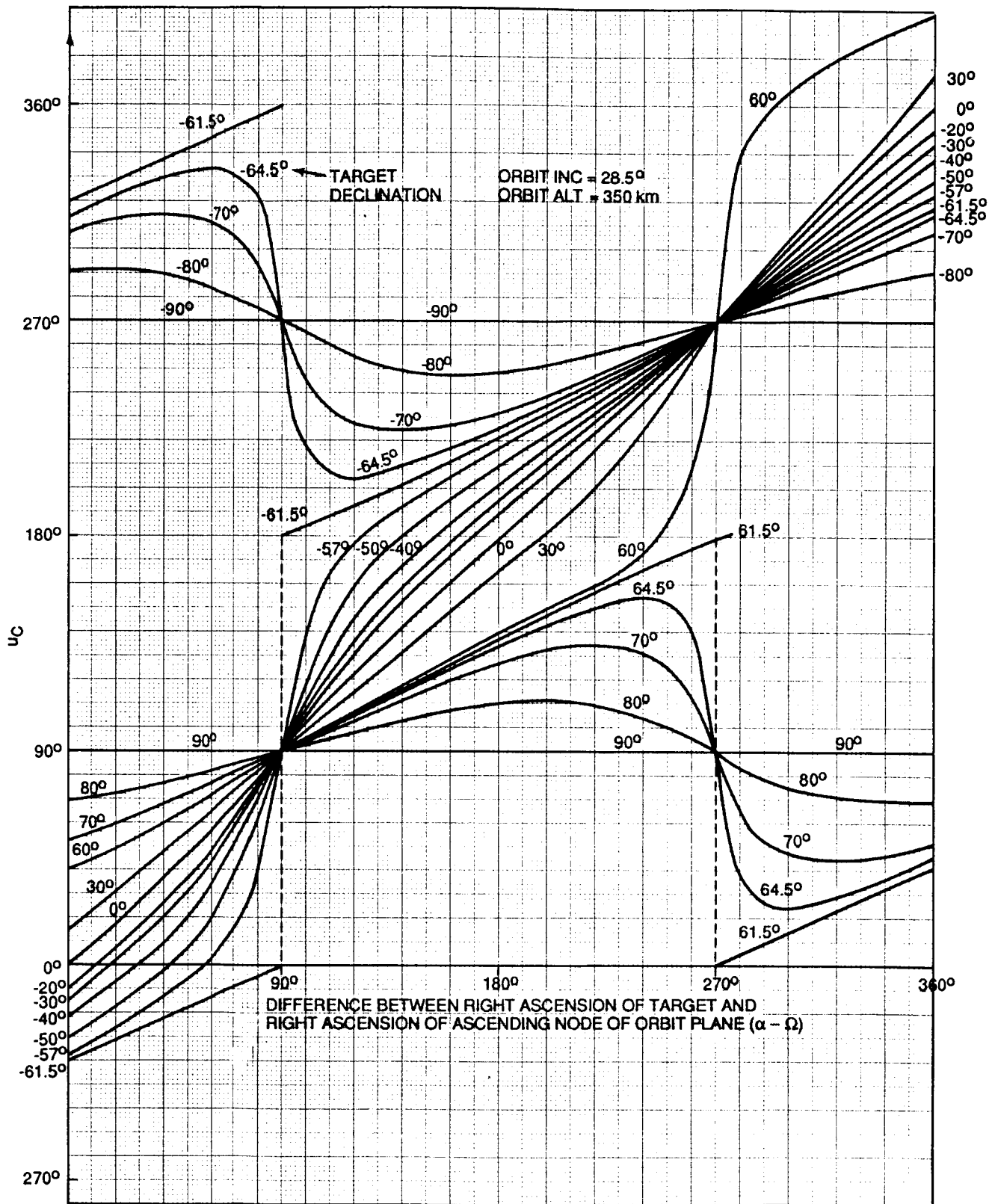


Figure 8. Argument of latitude of target culmination as a function of the difference between right ascension of target and right ascension of ascending node of orbit plane (target declination as parameter).

4, would be quite large, approaching 90° , and the observation time for either target by Figure 5 would be large for negative constraint OEA or small for positive constraint OEA.

For orbital parameters representative of the ASTRO-1 mission (i.e., $i = 28.^\circ 5$, $ALT = 350$ km) and a constraint orbital elevation angle of $1.^\circ 23$, Figure 9 presents the times of acquisition and loss as measured from the ascending node of an orbit (any orbit) for targets of varying declination and parametric values of $(\alpha-\Omega)$. Figure 9A shows $(\alpha-\Omega)$ parameterized from 0° to 180° in increments of 30° and Figure 9B shows $(\alpha-\Omega)$ parameterized from 180° to 360° in increments of 30° . This data was presented on two figures to keep one from becoming too cluttered to read conveniently. The constraint OEA of $1.^\circ 23$ resulted from the PI request to keep the line-of-sight to a target star at least 20° from the limb of the Earth combined with the limb of the Earth being about $18.^\circ 77$ below the local horizontal from a 350 km orbit.

The acquisition and loss time, relative to an ascending node, for any target anywhere on the celestial sphere can be read fairly accurately from these plots, certainly well enough to do preliminary mission planning. Consider, as an example, targets lying on the meridian plane defined by $\alpha-\Omega = 90^\circ$. Targets in this plane at all positive declinations and for negative declinations down to nearly -60° are acquired near the ascending node (0:00 time). For targets just below -60° declination (the orbit south pole) there is no acq/loss time because of the positive OEA constraint value of $1.^\circ 23$. Targets within $1.^\circ 23$ of the pole ($-61.^\circ 5 \pm 1.^\circ 23$) cannot be observed. Those at declinations more negative than about -63° are then acquired at the descending node of the orbit and lost at the following ascending node. The length of time that one of these targets can be observed is nearly 1/2 an orbital period except for those very near the orbital south pole. This is precisely what one would expect from the data presented in Figure 5. One can likewise tell very accurately from these charts the acquisition and loss time of any target on the celestial sphere for any orbit relative to its ascending node.

IV. SHIFT IN OBSERVABILITY WITH LAUNCH DELAY

A shift in the launch time of a mission, either earlier or later, will result in a shift (earlier or later) in the mission elapsed time (MET) at which a fixed object (star) can be observed from orbit. This is because a shift in launch time causes the orbit plane to be placed differently with respect to the "sky" (or the inertial coordinate system).

The shift in the acquisition and loss MET of a target due to a change in launch time is reflected by the change in the position of the culmination point of the target. The position of the culmination point was discussed in Section III and shown graphically in Figures 7 and 8. A launch delay caused the right ascension of the ascending node, Ω , to increase at a rate of $15^\circ/\text{hr}$; thus, the quantity of $(\alpha-\Omega)$ decreases at $15^\circ/\text{hr}$. This is shown by the bottom part of Figure 10. Figure 11 shows the change in $(\alpha-\Omega)$ as a function of launch delay for several starting values of $(\alpha-\Omega)$. For example, if originally $\alpha-\Omega = 60^\circ$ and one had a 2 hr launch delay, the new $\alpha-\Omega$ would be 30° . As can be seen from Figure 8, a target at 30° declination with these $(\alpha-\Omega)$ conditions would originally have a u_C of about 64° . With the 2 hr launch delay, u_C would decrease to about 40° . This would be a decrease of 24° . For an orbit mean motion

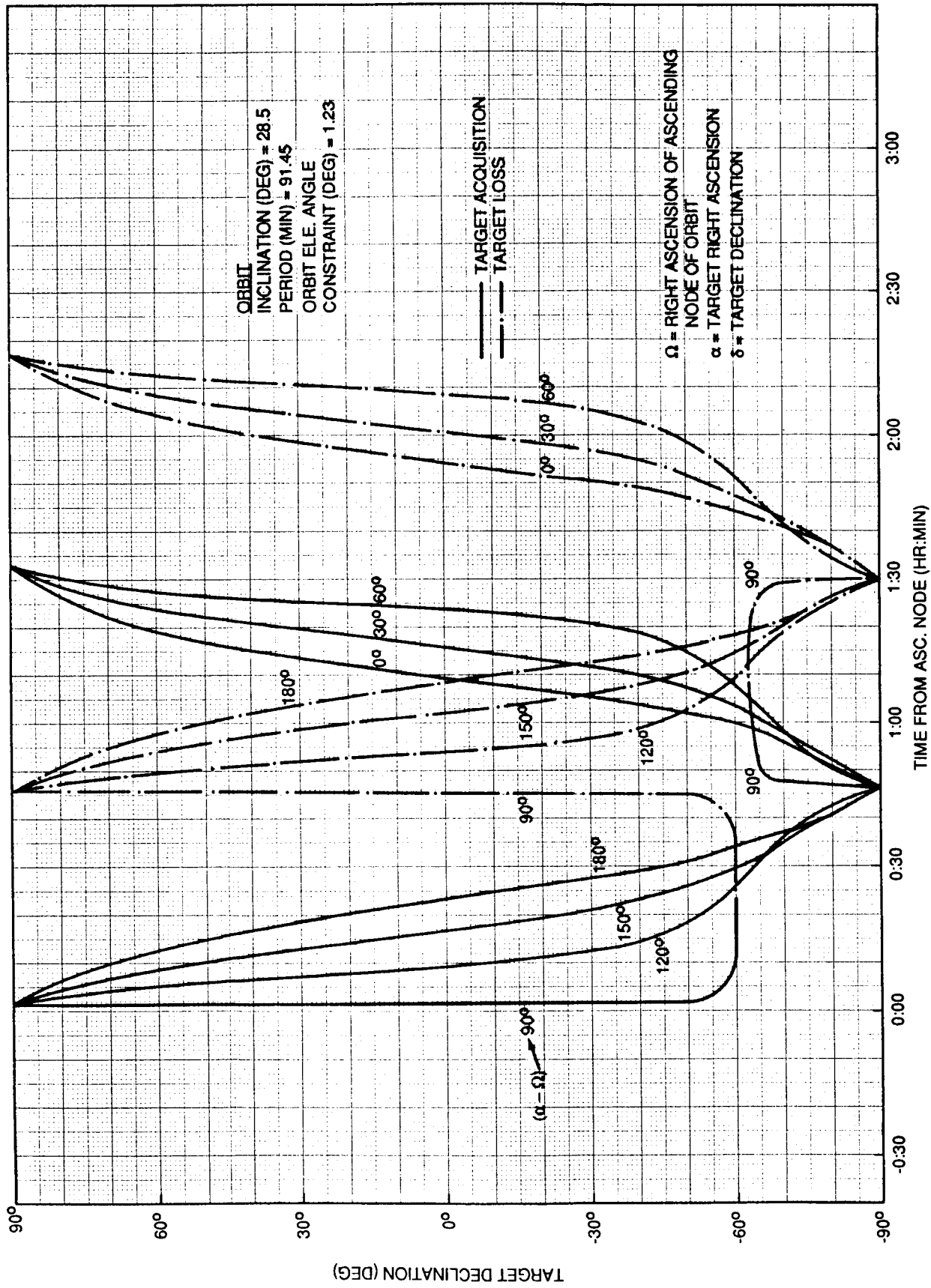


Figure 9A. Celestial target acq/loss times relative to orbit ascending node for varying target declinations.

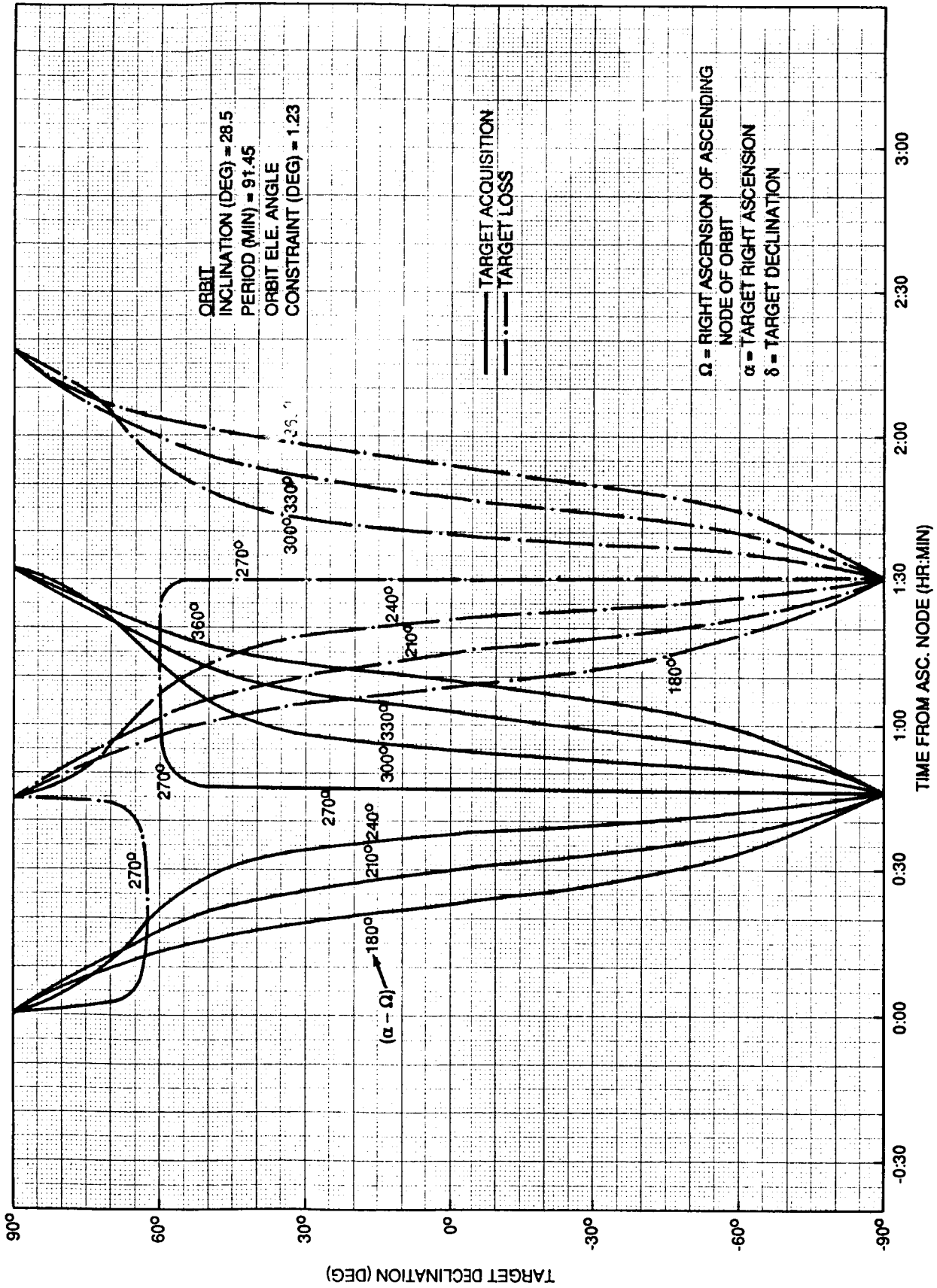


Figure 9B. Celestial target acq/loss times relative to orbit ascending node for varying target declinations.

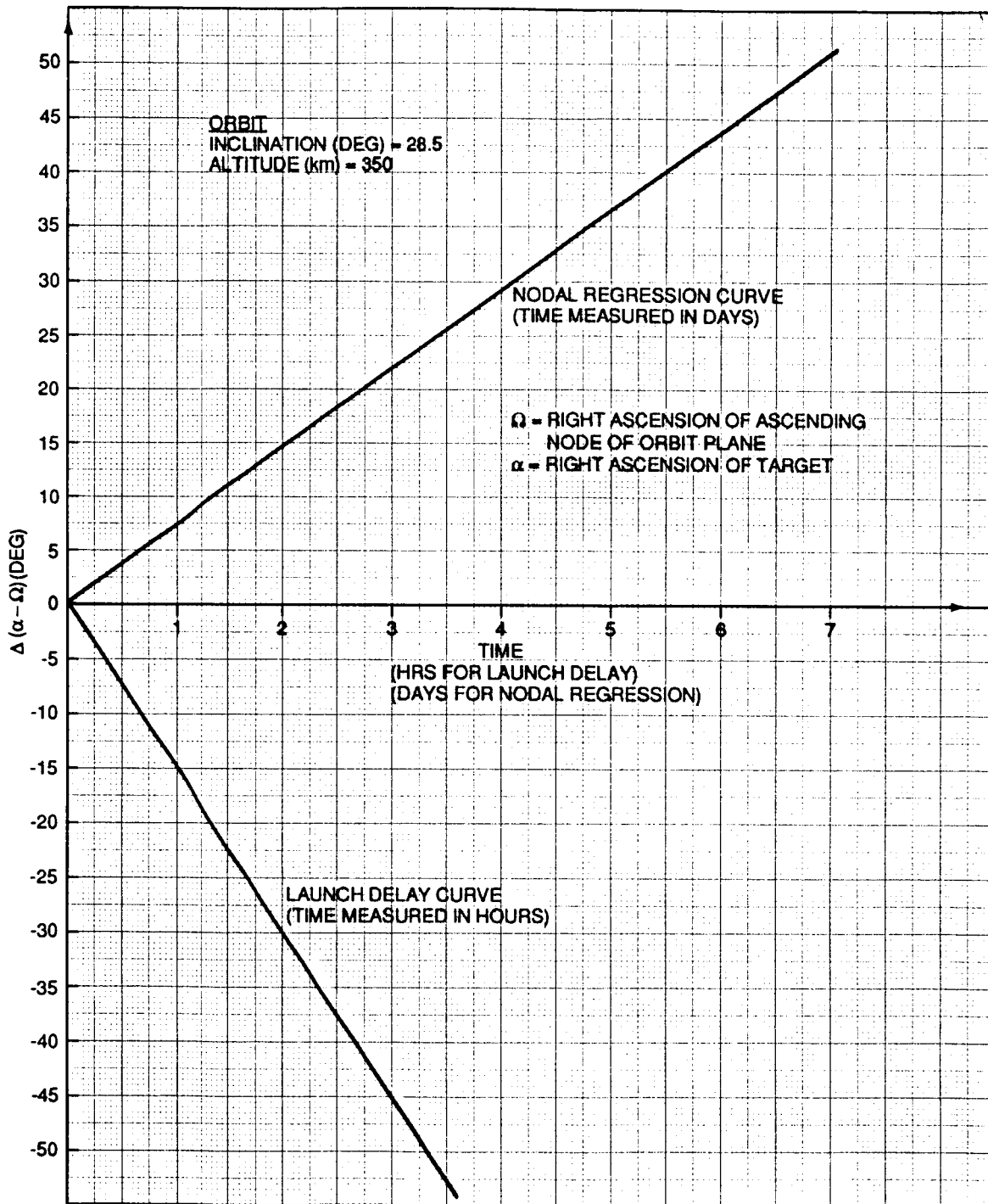


Figure 10. Effects of launch delay and nodal regression on angular difference between right ascension of target and right ascension of ascending node of orbit plane.

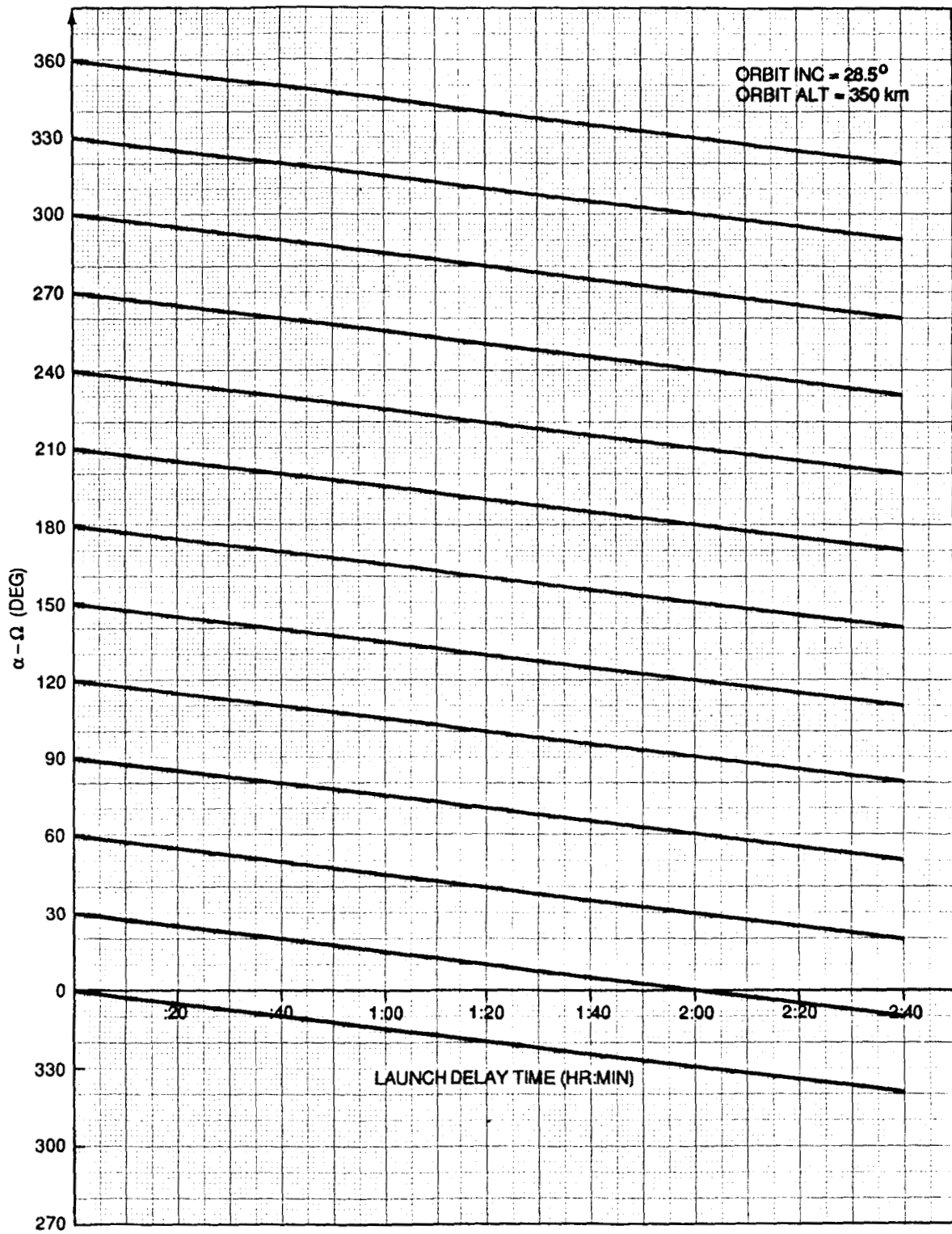


Figure 11. Effect of launch delay on target and orbit plane ascending node right ascension difference angle for various assumed initial values.

of 4°/min this would cause the acq/loss times of that target to occur 24/4 = 6 min earlier than for the nominal case. One can also see that shifts like this in many instances can cause the u_C to cross the value of 0° or be shifted into a previous orbit. The STAR computer program, which is used extensively by MSFC in mission planning work for astronomy missions, computes the acq/loss times in a given orbit based on which orbit the u_C falls in. Thus, one can sometimes see an acq/loss On/Off bar show a dramatic shift of one orbital period with a slight delay in launch time due to this phenomenon. This is not a basic or fundamental discontinuity; it is simply an artifact of the "bookkeeping" methods used within the computer program. This "jumping" is only apparent when one orbit of acq/loss data is computed in isolation. If many orbits are computed and shown consecutively, it is not seen.

The shift in the position of culmination as a function of change in launch time demonstrated by previous discussion and illustrated by Figure 7 and Figure 8 can be calculated from the equation

$$\Delta u_C = \frac{\partial u_C}{\partial LT} \Delta LT \quad , \quad (9)$$

where u_C is defined by equation (4). The orbital inclination i and the target coordinates α and δ remain constant with respect to change in LT and only Ω , the right ascension of the ascending node of the orbit plane is affected. Its rate of change is

$$\frac{\partial \Omega}{\partial LT} = \omega_e \quad [\omega_e = \text{the rotational rate of the earth}] \quad .$$

By direct differentiation it can be shown that

$$\frac{\partial u_C}{\partial LT} = -\omega_e (\cos \delta / \cos^2 \beta) * [\cos i \cos \delta + \sin i \sin \delta \sin (\alpha - \Omega)] \quad , \quad (10)$$

and it can be further shown that the quantity in brackets is $[\cos \beta (\partial \beta / \partial \delta)]$ where β is defined by equation (2). Thus, one can write

$$\frac{\partial u_C}{\partial LT} = -\omega_e \left[\begin{pmatrix} \cos \delta \\ \cos \beta \end{pmatrix} \begin{pmatrix} \partial \beta \\ \partial \delta \end{pmatrix} \right] \quad . \quad (11)$$

The direction of the shift in the observation time of a target with a delay in launch time then depends on the sign of the partial derivative, $\partial u_C / \partial LT$.

Furthermore, if one considers targets with a constant right ascension but with changing declinations, the shift in launch time of the targets with changing declination depends on the sign of the partial derivative $\partial \beta / \partial \delta$. The shift in launch time can be positive for some values of δ and negative for others. This has already been illustrated earlier during a discussion of the results shown in Figure 8. The cross-over point where the shift goes from positive to negative is where $\partial \beta / \partial \delta = 0$.

The zero point for this partial will occur at a declination given by differentiating the expression for β and setting it to zero.

$$\cos \beta \left(\frac{\partial \beta}{\partial \delta} \right) = \cos i \cos \delta + \sin i \sin \delta \sin (\alpha - \Omega) = 0 \quad (12)$$

or where

$$\delta = \tan^{-1} \left[\frac{-\cos i}{\sin i \sin (\alpha - \Omega)} \right] \quad (13)$$

The plot of the values of δ which satisfy this as a function of $(\alpha - \Omega)$ is shown in Figure 12.

Because $\partial u_C / \partial_{LT}$ has the opposite sign of $\partial \beta / \partial \delta$, then $\partial u_C / \partial_{LT}$ will be negative in the clear area of Figure 12. In that region an increase in launch time leads to a decrease in the acquisition time of a target, or it is acquired at an earlier MET. In the cross hatched regions of Figure 12, an increase in launch time leads to an increase in acquisition time of a target or it is acquired at a later MET than the nominal acquisition time. Figure 12 defines regions on the celestial sphere which are depicted on the diagram shown on Figure 13.

The shifts in the acquisition and loss METs of targets with a delay in launch time can be illustrated by the pair of diagrams in Figure 14. In the first diagram we consider two targets, each with right ascension 270° greater than that of the ascending node of the orbit plane. One of the targets, \hat{T}_1 , has a declination less than that of the orbital angular momentum vector \hat{J} ; i.e., less than $90^\circ - i$, while the second target, \hat{T}_2 , has a declination greater than that of \hat{J} , i.e., it lies in the cross hatched area of the celestial sphere shown in Figure 13. The culmination point of the \hat{T}_1 lies at an argument-of-latitude of 270° while that of \hat{T}_2 lies at an argument-of-latitude of 90° .

If one calculates the acquisition and loss times of these particular targets for an orbital elevation angle of 0° , then \hat{T}_1 is acquired at the descending node of the orbit plane and lost at the ascending node of the orbit plane. In other words, it will be visible during the entire southern hemisphere pass of the orbit. Target \hat{T}_2 will be exactly opposite. Its acquisition will occur at the ascending node and its loss will occur at the descending node. It will be visible during the entire northern hemisphere pass of the orbit.

The second figure in the pair shows the orbit plane relative to these same two targets after a launch delay of about an hour where the right ascension of the ascending node of the orbit plane has increased about 15° over that which it had in the first figure. In this case, the culmination of \hat{T}_1 [which occurs in the orbit plane where the target's position vector is projected onto the orbit plane by a great

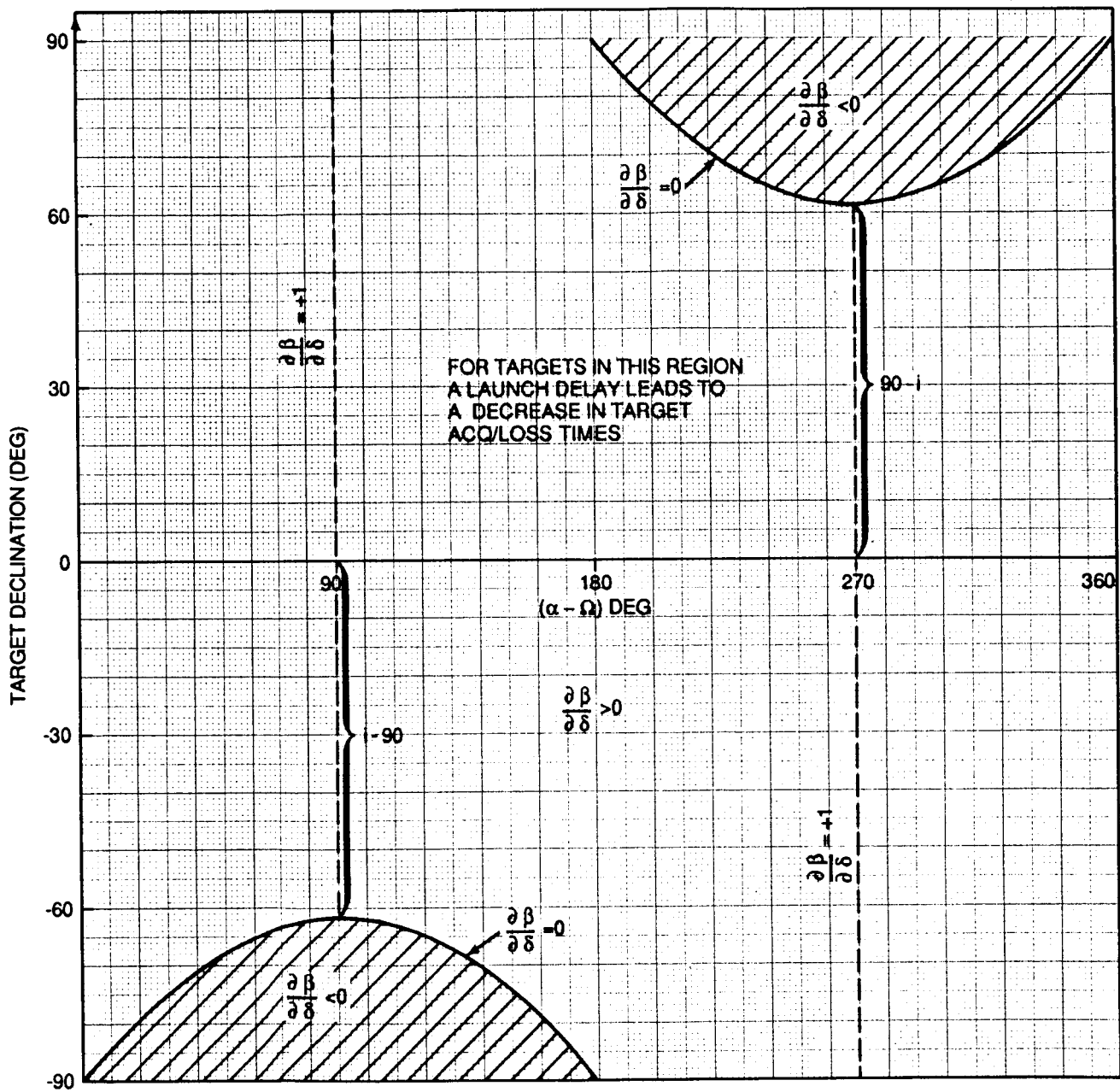


Figure 12. Regions on the celestial sphere where target acq/loss shift times change from negative to positive with a delay in launch time.

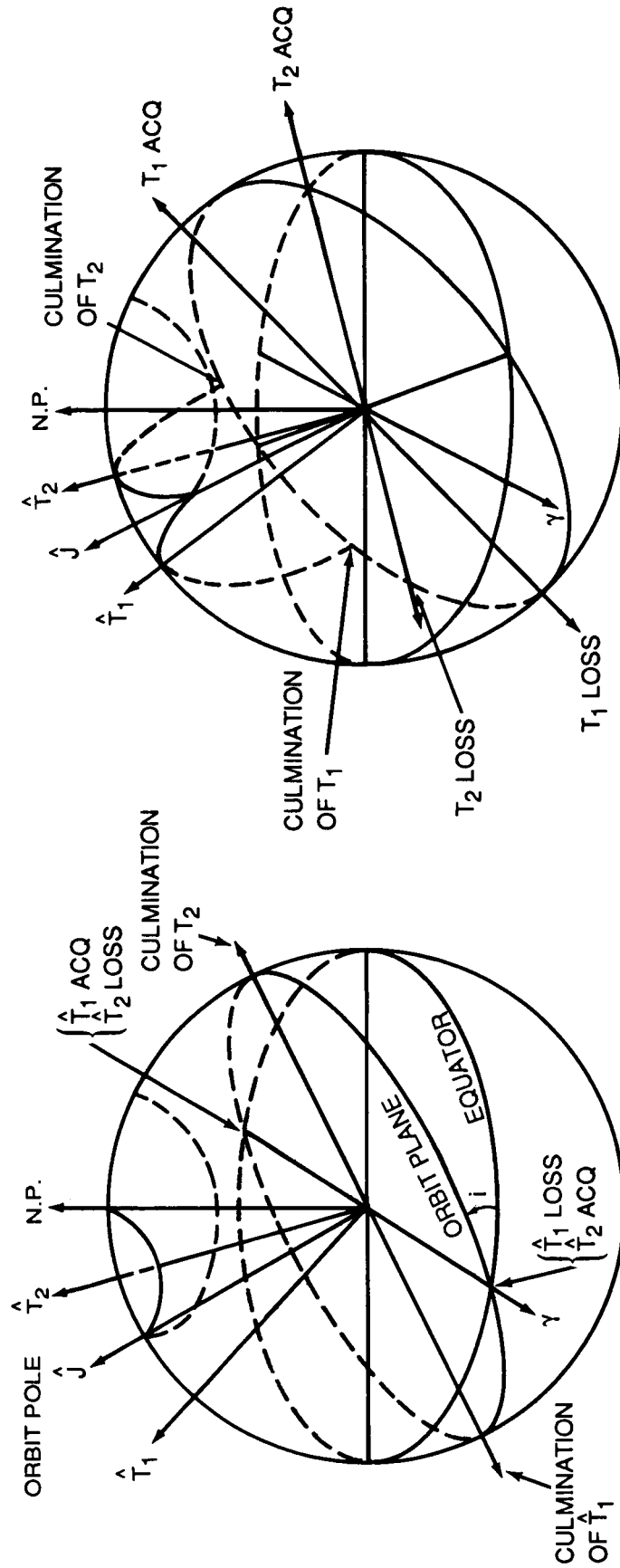


Figure 14. Illustration of acq/loss shift of targets on either side of the orbit pole with launch delay.

circle containing \hat{T}_1 and \hat{J} occurs at an argument of latitude of less than 270° . The acquisition and loss points which lie at 90° to either side of culmination occur at points prior to the descending and ascending nodes, respectively. A vehicle moving in this orbit plane would get to these points quicker (at an earlier MET) than it would have in the case shown by the first figure. Thus, the acq/loss times for \hat{T}_1 are shifted earlier than the nominal times by a delay in launch time.

The culmination of \hat{T}_2 now occurs at an argument-of-latitude greater than 90° . The acquisition and loss points of \hat{T}_2 now occur at points after the ascending and descending nodes, respectively. A vehicle moving in this orbit plane would get to these points later (at a later MET) than it would have in the case shown in the first figure. Thus, a delay in launch time causes the acq/loss times of \hat{T}_2 to be shifted later than those of the nominal launch time.

This geometrical picture confirms and gives insight into the earlier mathematical results.

V. SHIFT IN OBSERVABILITY WITH MISSION ELAPSED TIME

The relative position in the orbit plane where a celestial target is acquired and lost (u_A, u_L) gradually changes as the mission progresses. This is because the orbit plane slowly changes its position with respect to the celestial sphere; i.e., its line of nodes regresses due to the oblateness of the Earth. This regression rate is given by

$$\dot{\Omega} = -3/2 J_2 (r_e/a_o)^2 n_o \cos i \quad (14)$$

where $n_o = \sqrt{\mu/a_o^3}$ the mean motion, $\mu = 3.986012 \times 10^{14} \text{ m}^3/\text{s}^3$ and $J_2 = 1.0827 \times 10^{-3}$. a_o is the mean semi-major axis of the orbit and r_e is the equatorial radius of the Earth ($r_e = 6378160 \text{ m}$). Note that $\dot{\Omega}$ is a function of $\cos i$ and therefore goes to zero for polar orbits. This regression rate varies from about 7.5° per day for a $28^\circ.5$ inclined orbit to about $4.^\circ5/\text{day}$ for a 57° inclined orbit for low altitude orbits ($\sim 300 \text{ km alt.}$). This phenomenon produces an effect qualitatively the same as that of a launch delay but of smaller magnitude and in the opposite direction. A launch delay of 1 hr for example increases the right ascension of the ascending node by 15° over what it would have been for a launch on time, while an elapsed time of one day in orbit causes the right ascension of the node to decrease between $4.^\circ5$ and $7.^\circ5$ depending on the inclination and, to a lesser degree, the altitude.

The change in $(\alpha-\Omega)$ due to nodal regression for a $28.^\circ5$ inclined orbit is shown in the top half of Figure 10. Figure 15 shows some actual values of $(\alpha-\Omega)$ as a function of rev number or mission elapsed time for several starting or initial values of $(\alpha-\Omega)$. One could use this chart with a little interpolation to determine the value of $\alpha-\Omega$ at any point in a mission with any given starting value of $(\alpha-\Omega)$. One can then turn to the charts in Figures 9A or 9B to determine the acq/loss time of any target (relative to an ascending node) at any time point in the mission.

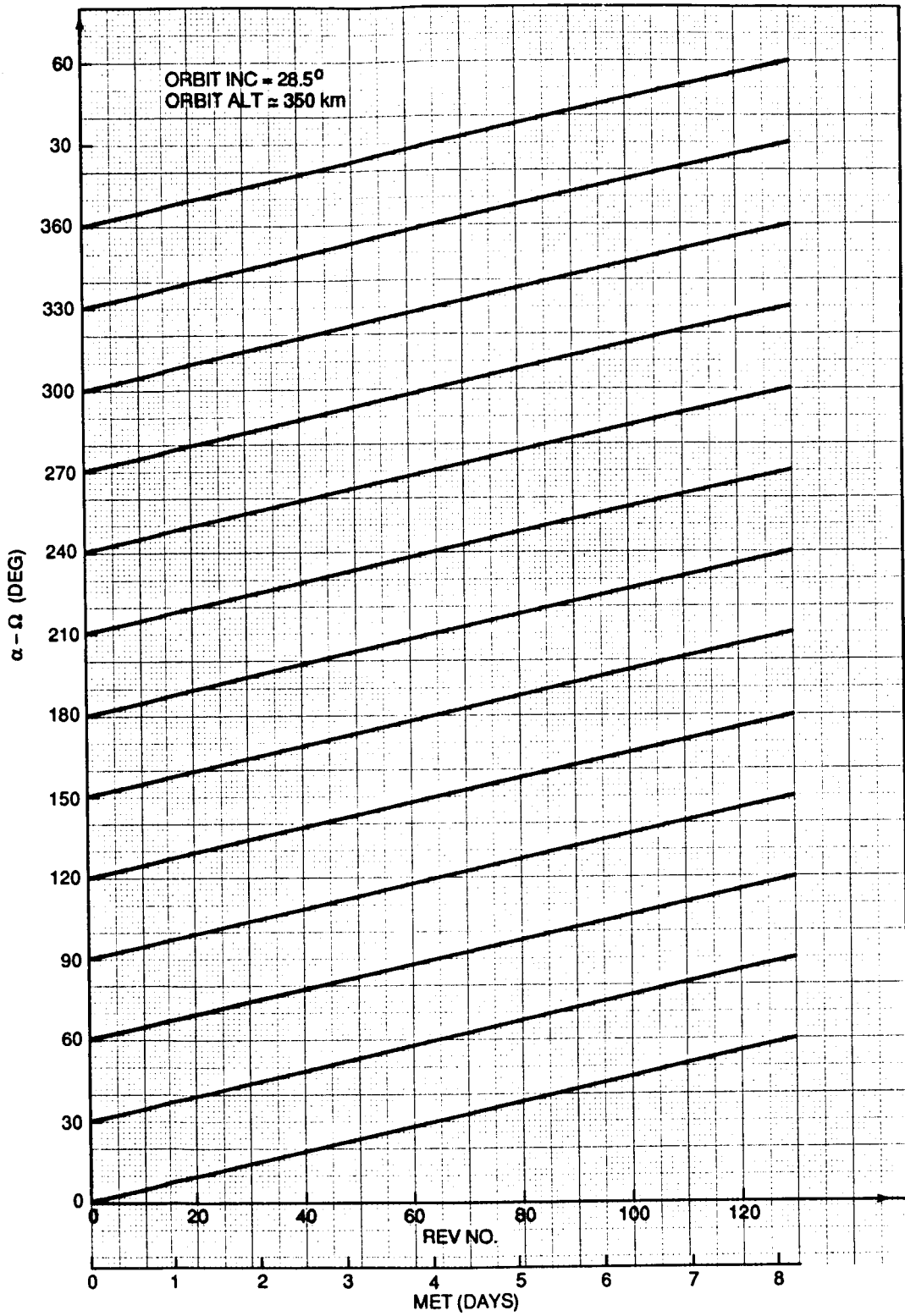


Figure 15. Effect of MET on target and orbit plane ascending node right ascension difference angle - various assumed initial values.

The acquisition and loss times of a target at a fixed place on the sky changes at a uniform rate with mission elapsed time due to the constant nodal regression rate (for a fixed orbit). As the position of the target is varied, however, the change in acquisition and loss times do not vary at a uniform rate with target position variation. Figures 7 and 8 showed the position of u_C (and consequently acquisition and loss times) as a function of $(\alpha-\Omega)$ and target declination. We will now calculate how rapidly this will change with variation of target position. The shift in the position of culmination (and consequently, acquisition and loss positions) with the passage of time can be calculated from the expression

$$\Delta u_C = \frac{\partial u_C}{\partial t} \cdot \Delta t \quad . \quad (15)$$

Using equation (4) for u_C , one can get by direct differentiation and some simplification that

$$\frac{\partial u_C}{\partial t} = -\dot{\Omega} \frac{\cos \delta}{\cos \beta} \frac{\partial \beta}{\partial \delta} \quad . \quad (16)$$

This has exactly the same form as $\partial u_C / \partial LT$ except that $\partial \Omega / \partial LT = \omega_e$ encountered in the former case, is here replaced by $\dot{\Omega}$ given by equation (14). Substituting equation (14) for $\dot{\Omega}$ and explicitly writing out $\partial \beta / \partial \delta$ gives

$$\frac{\partial u_C}{\partial t} = 3/2 J_2 \left(\frac{r_e}{a_o} \right)^2 n_o \cos i \frac{\cos \delta}{\cos^2 \beta} [\cos i \cos \delta + \sin i \sin \delta \sin (\alpha-\Omega)] \quad (17)$$

or

$$\frac{\partial u_C}{\partial t} = -\dot{\Omega} \frac{\cos \delta}{\cos^2 \beta} [\cos i \cos \delta + \sin i \sin \delta \sin (\alpha-\Omega)] \quad .$$

Because $\dot{\Omega}$, by equation (14), is always negative, the coefficient of $\partial \beta / \partial \delta$ in equation (16) will be positive for all δ and all β ; therefore, $\partial u_C / \partial t$ will have the same sign as $\partial \beta / \partial \delta$. The plot in Figure 12 shows where this partial is negative and where it is positive. Figure 13 then shows where targets lie on the celestial sphere for positive and negative shifts in acq/loss times with the passage of time.

Figure 16 shows a plot for equation (17) with δ as the independent variable, $\alpha-\Omega$ parameterized, and i fixed at $28.^\circ 5$.

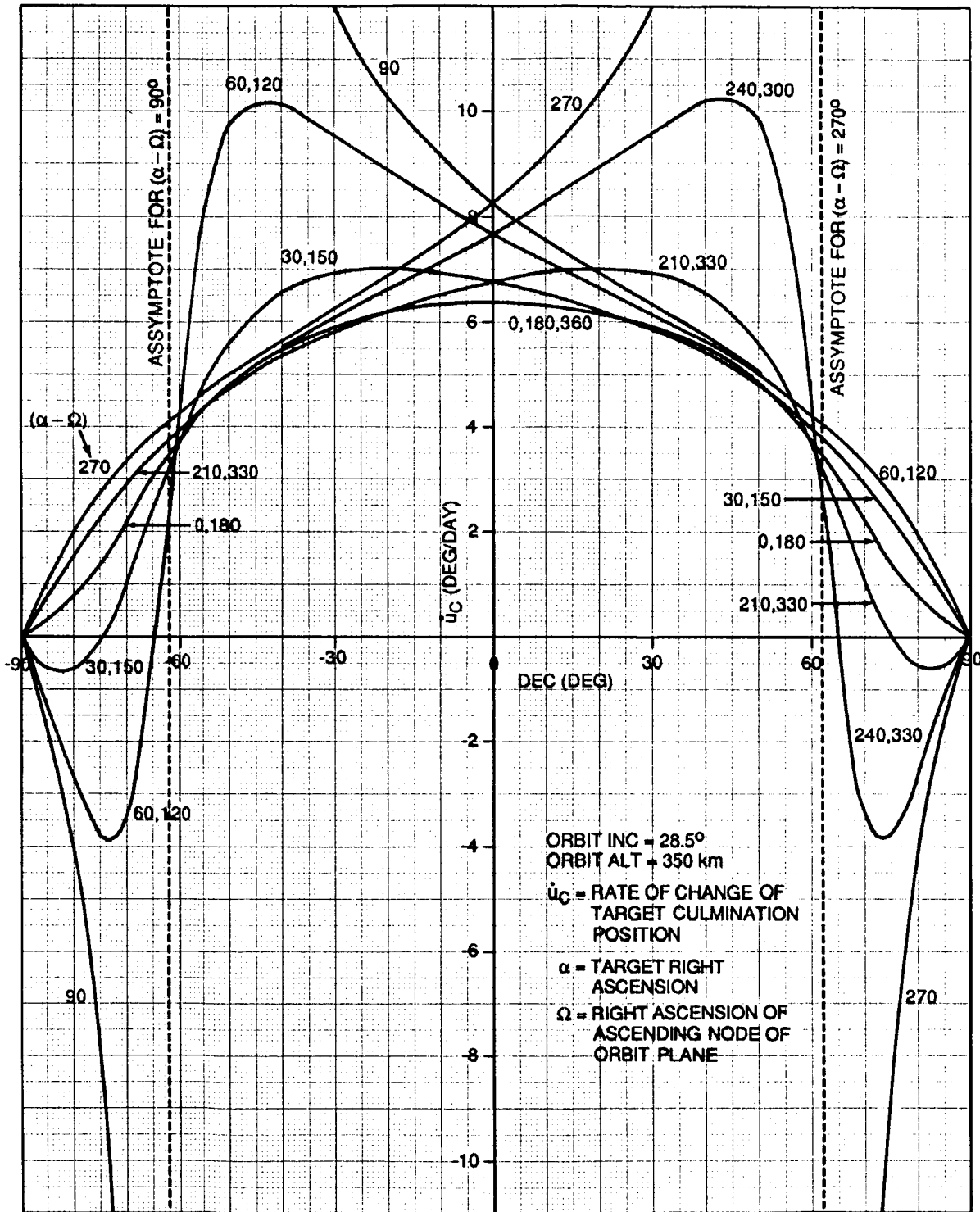


Figure 16. The rate of change of the culmination position in the orbit plane for targets of varying declination and various positions with respect to the orbital plane ($\alpha - \Omega$).

One can see from Figure 16 that for targets lying on the meridian plane defined by $\alpha - \Omega = 90^\circ$ there is a singularity at $\delta = -61.05$, the orbit south pole. For targets on this meridian plane lying at declination less negative than that of the orbit south pole \dot{u}_C is positive, indicating that these target acq/loss times shift forward in time or are acquired relatively later each revolution as time passes while targets with declinations more negative than that of the orbit south pole will shift backward or be acquired relatively earlier each revolution as time passes.

Four degrees of shift in the position of orbital noon translates into about 1 min of time shift in the acquisition and loss of a target; thus one can also use Figure 16 to estimate the time shift in the acq/loss of a target with elapsed time in the mission and also how rapidly it will change (and in what direction) with target position variation.

VI. SUN AND MOON INTERFERENCE

Celestial targets cannot be observed at will because of interference from extraneous objects in the line-of-sight (or near it) between the observing telescope and the observed objects. The Earth itself, is, of course, the major interfering body which has been discussed in the entirety of this report thus far. There are other sources of interference however. The major ones are the Sun and the Moon which will be discussed briefly. (Trapped radiation about the Earth represents a different type of interference for some instruments, and will not be discussed in this report.)

The Sun and/or the Moon represent an obstacle to viewing a celestial target only if they come too close in position to that object on the celestial sphere. The Sun moves in the ecliptic plane. This interference would be on an annual basis because of the apparent yearly motion of the Sun through the sky; i.e., for any given target there will be only a certain time of year (and the same time every year) when the Sun would interfere with observing it. This can be easily calculated from a given interference half-cone angle for any given target.

The angle between the Sun and target star is given by

$$\theta = \cos^{-1} (\hat{R}_\odot \cdot \hat{R}_*) = \cos^{-1} [\cos(\alpha_\odot - \alpha_*) \cos \delta_\odot \cos \delta_* - \sin \delta_\odot \sin \delta_*] \quad (18)$$

From spherical trigonometry and Figure 17 we can write

$$\sin \alpha_\odot = \frac{\tan \delta_\odot}{\tan \epsilon}$$

$$\cos L_\odot = \cos \alpha_\odot \cos \delta_\odot$$

$$\sin \delta_\odot = \sin \epsilon \sin L_\odot$$

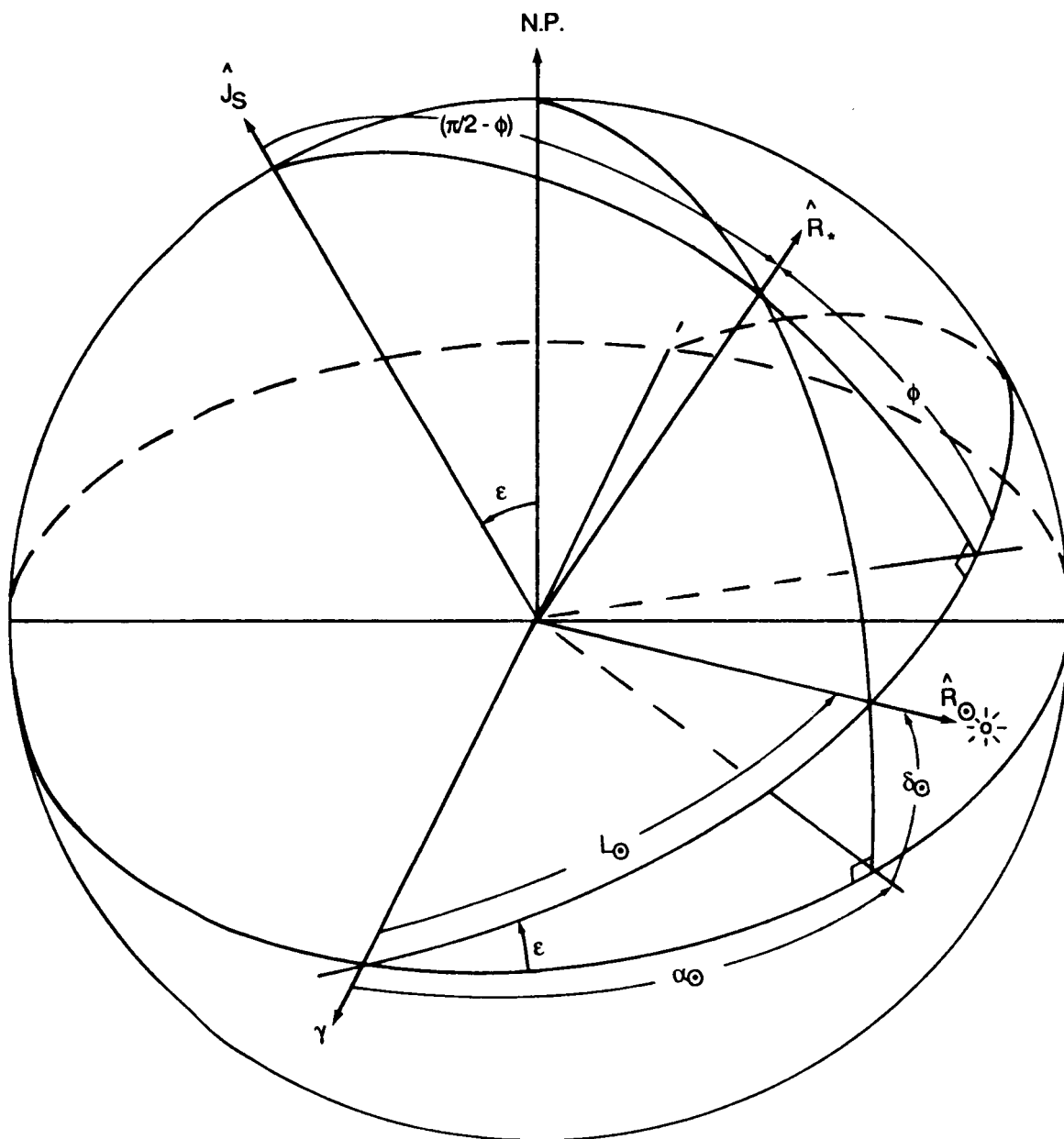


Figure 17. Illustration of Sun in ecliptic plane an angle ϕ of star to be observed out of ecliptic plane.

Where L_{\odot} is the mean longitude of the Sun in the ecliptic plane, which to a rough approximation is,

$$L_{\odot} = \dot{L} (t-t_0)$$

with $t_0 = \text{March 21}$ and $\dot{L} = 0.9856^{\circ}/\text{day}$. Expanding the equation for θ as

$$\begin{aligned} \cos \theta = & \cos \alpha_* \cos \delta_* [\cos \alpha_{\odot} \cos \delta_{\odot}] + \sin \alpha_* \cos \delta_* [\sin \alpha_{\odot} \cos \delta_{\odot}] \\ & + \sin \delta_* [\sin \delta_{\odot}] \quad , \end{aligned}$$

and substituting the above spherical trigonometry expressions for the quantities in the first and second brackets,

$$\cos \theta = \cos \alpha_* \cos \delta_* [\cos L_{\odot}] + \sin \alpha_* \cos \delta_* \left[\frac{\sin \delta_{\odot}}{\tan \epsilon} \right] + \sin \delta_* [\sin \delta_{\odot}] \quad .$$

Factoring $\sin \delta_{\odot}$ from the last two terms and substituting $\sin \epsilon \sin L_{\odot}$ for it and simplifying we get

$$\cos \theta = (\cos \alpha_* \cos \delta_*) \cos L_{\odot} + (\sin \alpha_* \cos \delta_* \cos \epsilon + \sin \delta_* \sin \epsilon) \sin L_{\odot} \quad . \quad (19)$$

Since θ is a constraint angle (constant), this equation has the form

$$a \cos L_{\odot} + b \sin L_{\odot} = c$$

with solution

$$L_{\odot \pm} = \tan^{-1} \left(\frac{b}{a} \right) \pm \cos^{-1} \left(\frac{c}{\sqrt{a^2 + b^2}} \right) \quad . \quad (20)$$

Since $L_{\odot} \sim \dot{L} (t-t_0)$, the time interval when the constraint is satisfied is given by,

$$t_{\pm} = t_0 + \left[\frac{L_{\odot \pm}}{\dot{L}} \right] \quad (21)$$

$$t_- = t_0 + \left[\frac{L_\ominus^-}{\dot{L}} \right] \quad (21)$$

(con.)

As an example: Let

$$\begin{aligned} \alpha_* &= 90^\circ & \epsilon &= 23.^\circ 5 \\ \delta_* &= 23.^\circ 5 & \theta &= 30^\circ \end{aligned}$$

Then

$$a = 0 \quad , \quad b = 1.0 \quad , \quad c = 0.866$$

$$L_\pm = 90^\circ \pm 30^\circ$$

$$L_- = 60^\circ$$

$$L_+ = 120^\circ$$

$$t_- = \text{March 21} + \frac{60^\circ}{0.9856^\circ/\text{day}} \cong \text{March 21} + 61 \text{ days} \cong \text{May 21}$$

$$t_+ = \text{March 21} + \frac{120^\circ}{0.9856^\circ/\text{day}} \cong \text{March 21} + 122 \text{ days} \cong \text{July 21}$$

Thus, a target at $(\alpha, \delta) = (90^\circ, 23.^\circ 5)$ with a constraint angle of 30° from the Sun could not be viewed from about May 21 to July 21 on any year. This example is, of course, obvious from inspection.

If the target star is out of the ecliptic plane by more than the half-cone interference angle θ then the Sun will never interfere with the observation of the target star. The distance ϕ that the target star is out of the ecliptic plane is illustrated in Figure 17 and can be calculated from

$$\begin{aligned} \hat{R}^* \cdot \hat{J}_s &= \cos(\pi/2 - \phi) = \sin \phi \\ &= \cos \epsilon \sin \delta_* - \sin \alpha_* \cos \delta_* \sin \epsilon \end{aligned} \quad (22)$$

If $|\phi| > \theta$ There will never be any interference from the Sun and in this case equation (20) would have no solutions.

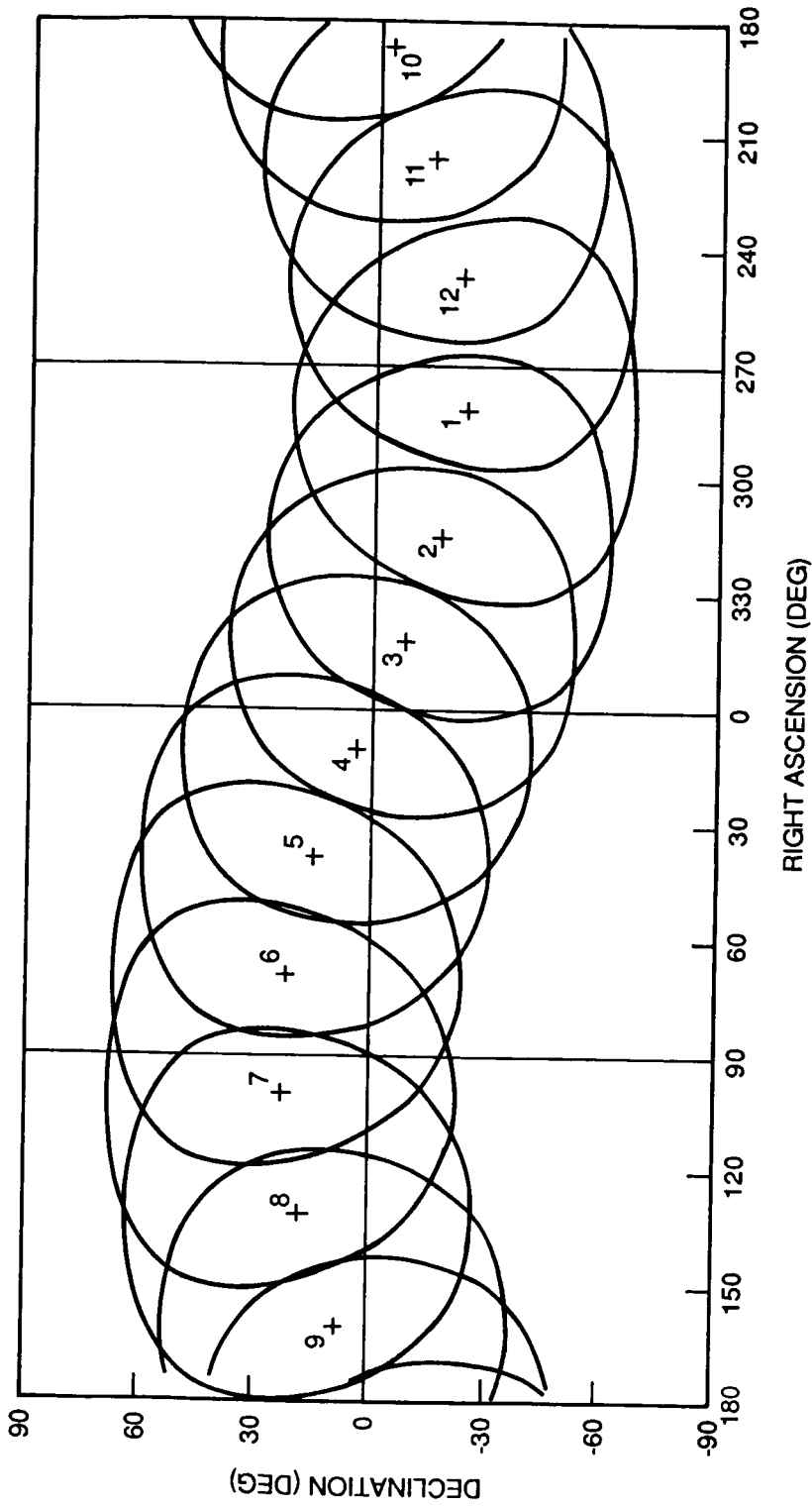
Figure 18 shows the position of the Sun on the celestial sphere on the first day of each month for a whole year with a 45° constraint angle (half-cone angle) about each position which is the specified solar avoidance angle for ASTRO-1. This position marked 1 is for January 1, the position marked 2 is for February 1, and so on for each month of the year. For any given time of the year, then, one can tell fairly accurately from this chart where the Sun is and what the avoidance region for that time of year will be.

Interference from the Moon is a much more difficult case to give a simple approximate equation for because of the complexity of the moon's motion. Its orbit plane is inclined at about 5.1° to the ecliptic plane. The right ascension of its ascending node oscillates between about $\pm 13^\circ$ about the vernal equinox with a period of about 18 years. Its sidereal period about the Earth is about 27.3 days. If there is interference from the Moon it will occur on a monthly basis rather than an annual basis as with the Sun. The usual practice in mission planning is to launch near "new Moon" so that the Sun and Moon are in the same part of the sky and give only one area of interference. This has the additional benefit of giving dark night skies for observations.

Figure 19 shows the position of the Moon on the celestial sphere over a period of about one month with the position of the Moon shown at three day intervals. The lunar positions shown on this Figure were generated for early 1989. The position marked 1 (near 0° right ascension and 0° declination) is for January 13, 1989; the position marked 2 is for January 16, 1989; 3 is for January 19, 1989, and so on. The final position marked 10 is for February 9, 1989. The large circle around each lunar position is a 45° lunar avoidance area for night-time target scheduling and the small circle is a 20° lunar avoidance area for day-time target scheduling. This movement of the moon relative to inertial space repeats itself every 27.321 days. For example, the Moon has 0° right ascension on January 12, 1989 at about 22.2 hrs GMT; then 27.321 days later on February 9, 1989, at about 6.0 hrs GMT the Moon is again at 0° right ascension and so on. By continually adding 27.321 days to the previous date one can get approximate times every month for the Moon's starting position on the chart. Continuing this indefinitely will gradually lead to sizeable errors, but for the years 1989 and 1990 the following table gives the approximate times when the moon will be at 0° right ascension.

Approximate Dates in 1989 and 1990 when the
Moon will be at 0° Right Ascension

<u>1989</u>		<u>1990</u>	
<u>Day</u>	<u>Hour (GMT)</u>	<u>Day</u>	<u>Hour (GMT)</u>
Jan. 12	22.2	Jan. 3	13.7
Feb. 9	6.0	Jan. 30	19.4
Mar. 8	16.7	Feb. 27	3.0
Apr. 5	3.5	Mar. 26	12.8
May 2	14.0	Apr. 22	22.5
May 29	22.0	May 20	9.8
June 26	3.5	June 16	17.2
July 23	9.0	July 13	22.9
Aug. 19	16.6	Aug. 10	4.4
Sept. 16	2.5	Sept. 6	11.6
Oct. 13	13.0	Oct. 3	20.9
Nov. 10	0.0	Oct. 31	7.5
Dec. 7	8.3	Nov. 27	17.8



SOLAR AVOIDANCE ANGLE = 45°

- 1 = JAN. 1
- 2 = FEB. 1
- ...
- 12 = DEC. 1

Figure 18. The solar position and the region of solar avoidance over an annual cycle.

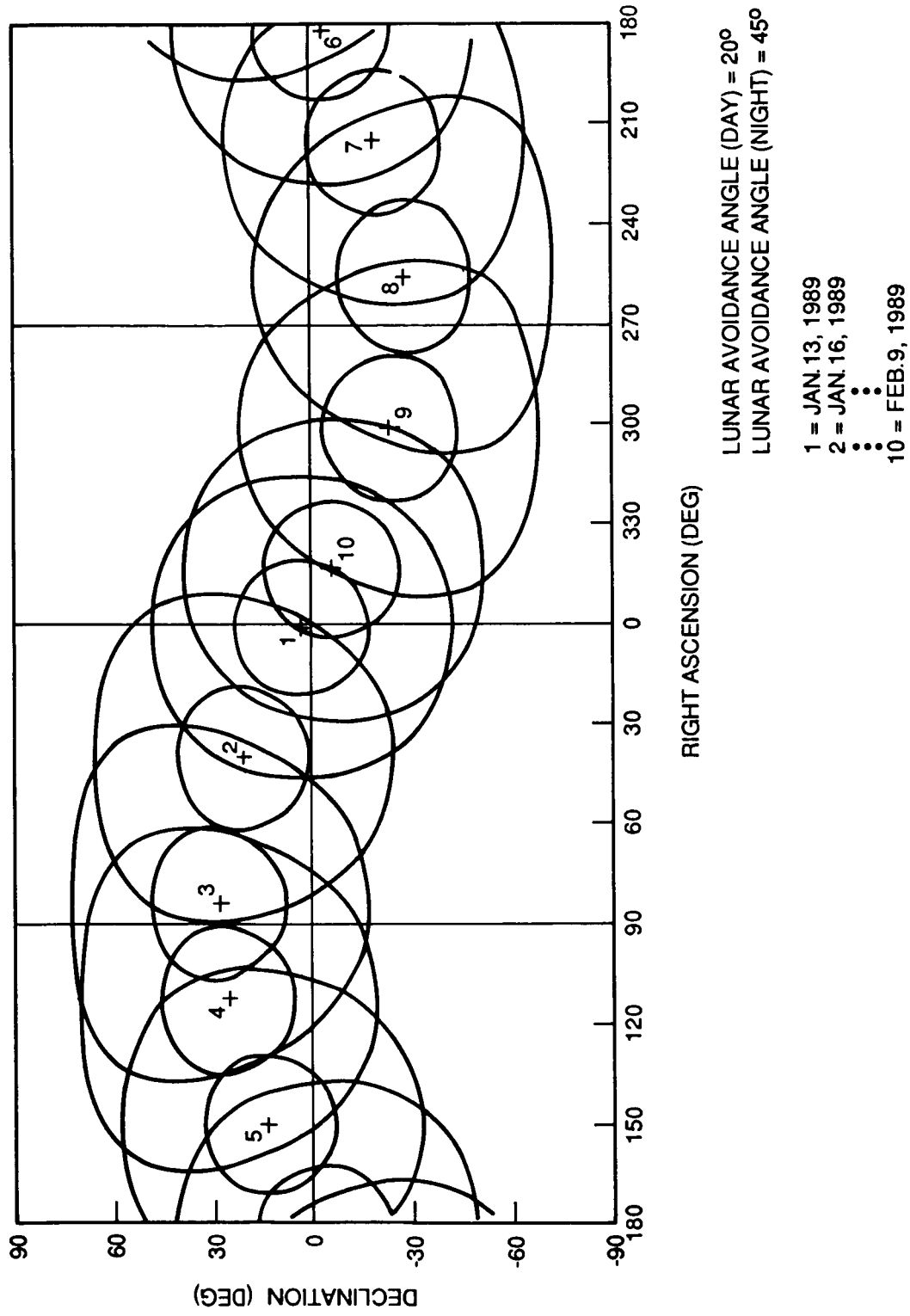


Figure 19. The lunar position with the day-time and night-time lunar avoidance regions shown for a one-month time period.

APPENDIX A

DERIVATION OF BETA ANGLE, ARGUMENT-OF-LATITUDE OF CULMINATION, AND ORBITAL ELEVATION ANGLE

The unit angular momentum vector of the orbit (which is the orbit pole) illustrated by Figure 3, is given by

$$\hat{J} = \hat{i} (\sin i \sin \Omega) + \hat{j} (-\sin i \cos \Omega) + \hat{k} (\cos i) \quad . \quad (A-1)$$

A unit vector to a star with right ascension α_* and declination δ_* is

$$\hat{R}^* = \hat{i} (\cos \alpha_* \cos \delta_*) + \hat{j} (\sin \alpha_* \cos \delta_*) + \hat{k} (\sin \delta_*) \quad . \quad (A-2)$$

(See Figure 3 for an illustration of these vectors.) By definition, the β -angle of the star is the angle between the vector to the star and the projection of that vector onto the orbit plane. This is also illustrated in Figure 3. Mathematically the β -angle is calculated as

$$\hat{R}^* \cdot \hat{J} = \cos (90 - \beta^*) = \sin \beta^* \quad . \quad (A-3)$$

Using equations (A-1) and (A-2) to construct the scalar product indicated in equation (A-3) gives the following result for the angle

$$\beta^* = \sin^{-1} [\cos i \sin \delta_* - \cos \delta_* \sin i \sin (\alpha_* - \Omega)] \quad . \quad (A-4)$$

By convention, the β -angle is positive if the star is on the same side of the orbit plane as \hat{J} and negative otherwise.

The culmination of a star is the place in the orbit plane where the star attains its maximum elevation angle above the local horizontal plane. This occurs in the orbit plane where the star's position vector is projected onto the orbit plane by a great circle containing \hat{R}^* and \hat{J} . This position in the orbit plane, measured from the ascending node of the orbit, is called the argument of latitude of culmination, u_C .

The argument of latitude of culmination can be calculated as follows: A point in the orbital plane 90° from orbital noon in the direction of orbit travel (which would be the terminator for the star on the surface of the Earth), which is called R_{GT}^* , is calculated as

$$\hat{J} \times \hat{R}^* = |\hat{J}| |\hat{R}^*| \sin (90^\circ - \beta^*) \hat{R}_{GT}^* = \cos \beta^* \hat{R}_{GT}^* \quad (A-5)$$

or

$$\begin{aligned} \hat{R}_{GT}^* = \frac{\hat{J} \times \hat{R}^*}{\cos \beta^*} = & [\hat{i} (-\sin i \cos \Omega \sin \delta_* - \cos i \sin \alpha_* \cos \delta_*) \\ & + \hat{j} (\cos i \cos \alpha_* \cos \delta_* - \sin i \sin \Omega \sin \delta_*) \\ & + \hat{k} (\sin i \cos \delta_* \sin (\alpha_* - \Omega))] / \cos \beta^* \end{aligned} \quad (A-6)$$

Let a unit vector to the ascending node of the orbit plane be denoted by \hat{P} ; i.e.,

$$\hat{P} = \hat{i} (\cos \Omega) + \hat{j} (\sin \Omega) + \hat{k}(0) \quad . \quad (A-7)$$

The argument of latitude of the star-set terminator u_{SST}^* can be calculated from

$$u_{SST}^* = \cos^{-1} (\hat{R}_{GT}^* \cdot \hat{P}) = \cos^{-1} \left[\frac{-\sin i \sin \delta_* - \cos i \cos \delta_* \sin (\alpha_* - \Omega)}{\cos \beta^*} \right] \quad (A-8)$$

The argument of latitude of culmination is 90° less than the argument of latitude of the star-set terminator; i.e.,

$$u_C^* = u_{SST}^* - 90^\circ \quad . \quad (A-9)$$

Therefore

$$\sin u_C^* = \sin (u_{SST}^* - 90^\circ) = -\cos u_{SST}^* \quad . \quad (A-10)$$

Combining equations (A-8) and (A-10) gives

$$\sin u_C^* = \frac{\sin i \sin \delta_* + \cos i \cos \delta_* \sin (\alpha_* - \Omega)}{\cos \beta^*} \quad . \quad (A-11)$$

It is also necessary to have an expression for $\cos u_C^*$ in order to determine u_C^* without any ambiguity as to quadrant.

A unit vector to culmination, \hat{R}_C^* , is

$$\hat{R}_C^* = \hat{R}_{GT}^* \times \hat{J} = \frac{(\hat{J} \times \hat{R}^*) \times \hat{J}}{\cos \beta^*} = \frac{-1}{\cos \beta^*} [\hat{J} (\hat{J} \cdot \hat{R}^*) - \hat{R}^* (\hat{J} \cdot \hat{J})]$$

or

$$\hat{R}_C^* = - \frac{1}{\cos \beta^*} [\hat{J} (\sin \beta^*) - \hat{R}^*] \quad . \quad (A-12)$$

Then,

$$\hat{P} \cdot \hat{R}_C^* = \cos u_C^* \quad , \quad (A-13)$$

substituting equations (A-7) and (A-12) into equation (A-13) gives

$$\cos u_C^* = - \frac{1}{\cos \beta^*} [\sin \beta^* (\hat{P} \cdot \hat{J}) - \hat{R}^* \cdot \hat{P}] \quad (A-14)$$

but $\hat{P} \cdot \hat{J} = 0$, therefore

$$\cos u_C^* = \frac{1}{\cos \beta^*} [\hat{P} \cdot \hat{R}^*] = \frac{1}{\cos \beta^*} [\cos \delta_* \cos (\alpha_* - \Omega)] \quad . \quad (A-15)$$

From equations (A-11) and (A-15) one then gets

$$u_C^* = \tan^{-1} \left(\frac{\sin u_C^*}{\cos u_C^*} \right) = \tan^{-1} \left[\frac{\sin i \sin \delta_* + \cos i \cos \delta_* \sin (\alpha_* - \Omega)}{\cos \delta_* \cos (\alpha_* - \Omega)} \right] \quad (A-16)$$

The radius vector of the vehicle points to the local zenith which is 90° from the local horizontal plane. By definition, the orbital elevation angle, OEA, of a star from the local horizontal is

$$\text{OEA} = 90^\circ - \cos^{-1} (\hat{R}_V \cdot \hat{R}^*) \quad (A-17)$$

The unit vector to the star \hat{R}^* is given by equation (A-2). The unit vector to the vehicle is

$$\begin{aligned} \hat{R}_V = & \hat{i} (\cos \Omega \cos u - \sin \Omega \cos i \sin u) \\ & + \hat{j} (\sin \Omega \cos u + \cos \Omega \cos i \sin u) + \hat{k} (\sin i \sin u) \quad . \quad (A-18) \end{aligned}$$

Rewriting (A-17), we get

$$90^\circ - \text{OEA} = \cos^{-1} (\hat{R}_V \cdot \hat{R}^*)$$

or $\cos (90^\circ - \text{OEA}) = \sin (\text{OEA}) = (\hat{R}_V \cdot \hat{R}^*)$

$$\text{OEA} = \sin^{-1} (\hat{R}_V \cdot \hat{R}^*) \quad . \quad (\text{A-19})$$

Substituting equations (A-2) and (A-18) into equation (A-19) gives

$$\begin{aligned} \text{OEA} = \sin^{-1} \{ & \cos u [\cos \delta_* \cos (\alpha_* - \Omega)] + \sin u [\cos \delta_* \cos i \sin (\alpha_* - \Omega) \\ & + \sin \delta_* \sin i] \} \quad . \quad (\text{A-20}) \end{aligned}$$

One can substitute equation (A-15) for the coefficient of $\cos u$ into equation (A-20), and equation (A-11) for the coefficient of $\sin u$ into equation (A-20) to get

$$\text{OEA} = \sin^{-1} \{ \cos u [\cos u_C^* \cos \beta^*] + \sin u [\sin u_C^* \cos \beta^*] \}$$

which simplifies to

$$\text{OEA} = \sin^{-1} [\cos \beta^* \cos (u_C^* - u)] \quad . \quad (\text{A-21})$$

The angles β^* and u_C^* calculated in equations (A-4) and (A-16) change very slowly and can be considered constant for one orbit. Thus, equation (A-21) can be used to calculate the orbital elevation angle of a given star from any point u in the orbit. u can be varied arbitrarily from 0° to 360° to obtain the elevation angle at any point in the orbit. The OEA will vary between the limits $\pm |90 - \beta^*|$.

Conversely, equation (A-21) can be inverted to calculate the argument of latitude u required for a star to obtain a given OEA.

$$u_{A,L}^* = u_C^* \mp \cos^{-1} \left[\frac{\sin (\text{OEA})}{\cos \beta^*} \right] \quad (\text{A-22})$$

The minus sign gives the argument of latitude of acquisition while the plus sign gives the argument of latitude of loss. OEA can be chosen arbitrarily between the physically meaningful limits of $\pm 90^\circ$. In practice, it is chosen to satisfy some physical or scientific constraint. The observation time per orbit above a given OEA is

$$OT = 2^* \cos^{-1} \left[\frac{\sin(OEA)}{\cos \beta^*} \right] / \dot{u} \quad . \quad (A-23)$$

\dot{u} in equation (A-23) is the orbital mean motion of the vehicle; expressed in degrees per minutes gives the OT in minutes; expressed in degrees per hour gives the OT in hours.

The time from the ascending node that the star is acquired and lost is

$$T_{ACQ}^* = u_A^* / \dot{u} \quad ; \quad T_{LOSS}^* = u_L^* / \dot{u} \quad (A-24)$$

The mission elapsed time (MET) of acquisition and loss is obtained by adding the time of the ascending node to the above times

$$MET_{ACQ}^* = MET_{NODE} + T_{ACQ}^*$$

$$MET_{LOSS}^* = MET_{NODE} + T_{LOSS}^* \quad . \quad (A-25)$$

If a minimum OEA is known or given, it can be substituted directly into equation (A-22). If the constraint is expressed as having the line-of-sight from the orbiting vehicle to the star pass through the atmosphere at an altitude not lower than ALT_A and the vehicle is at an altitude of ALT_O , then the minimum OAE is calculated as

$$OEA = \cos^{-1} \left(\frac{R_E + ALT_A}{R_E + ALT_O} \right) \quad . \quad (A-26)$$

This is illustrated in Figure A-1. A negative sign is given to OEA when ALT_A is less than ALT_O . The elevation angle of the limb of the Earth is calculated from equation (A-26) by letting $ALT_A = 0$. From an altitude of 350 km, for example, the limb of the Earth is at an elevation angle of ≈ -18.56 .

If the viewing telescope has an FOV of X° and the bottom edge of the FOV should not come closer than ALT_A to the limb of the Earth, then the minimum OEA is that calculated by equation (A-26) and then adding $(X/2)^\circ$ to the result.

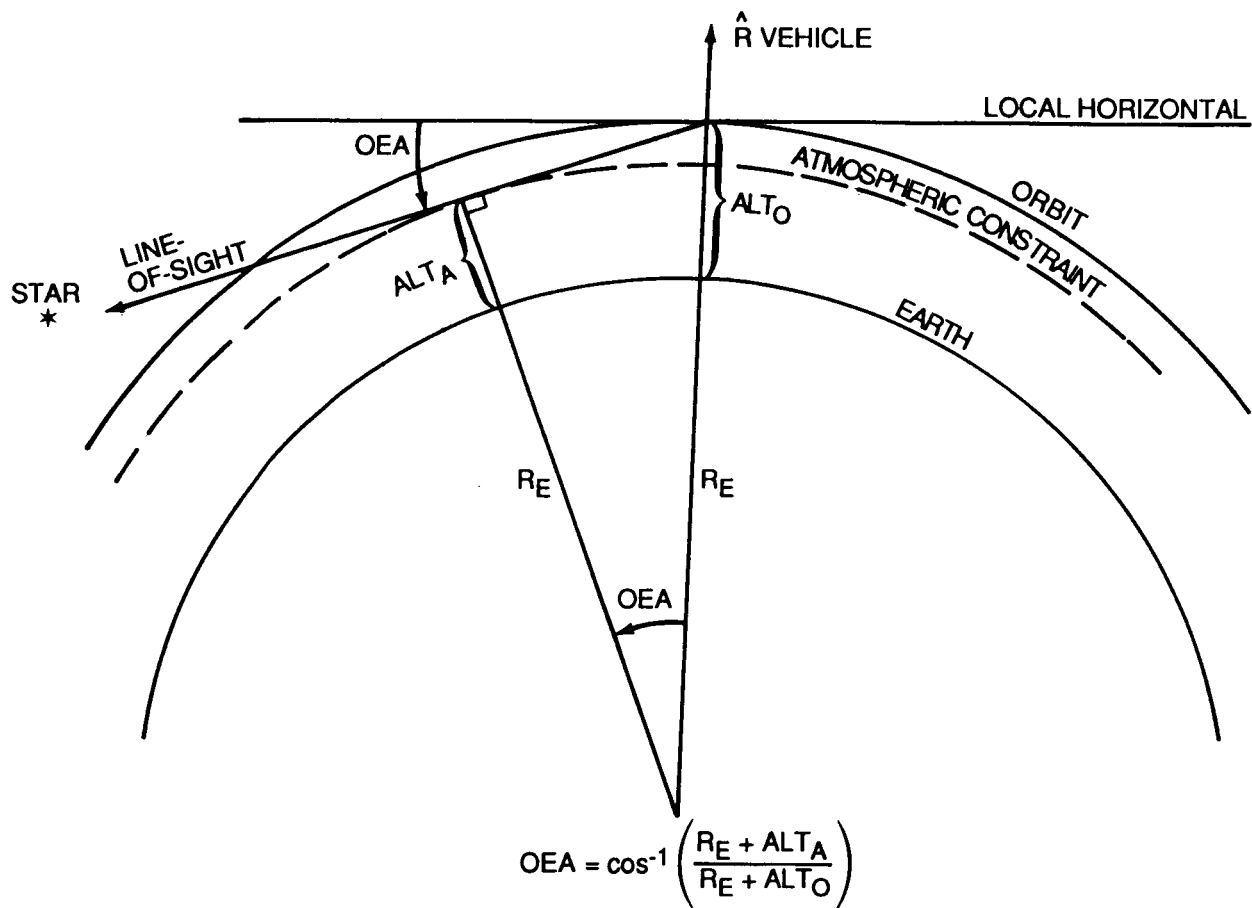


Figure A-1. Illustration of minimum OEA for a given atmospheric constraint.

APPENDIX B

CALCULATING THE RIGHT ASCENSION OF THE ASCENDING NODE OF THE ORBIT PLANE

In order to maximize the usefulness of the equations presented in the body of this report, it is necessary for a user to be able to determine the right ascension of the ascending node of an orbit plane. This appendix gives an approximate way of doing this. It will be accurate enough for feasibility analyses.

The right ascension of the ascending node at any time after insertion at time t_0 is given by

$$\Omega = \Omega_0 + \dot{\Omega} (t-t_0) \quad (\text{B-1})$$

where $\dot{\Omega}$, the regression rate of the line of nodes, is given to first order by

$$\dot{\Omega} = -3/2 J_2 (r_e/a(1-e^2)) n_0 \cos i \quad (\text{B-2})$$

and where

r_e = Earth's equatorial radius (6378160 meters)

a = semi-major axis of orbit

e = eccentricity of orbit

i = inclination of orbit

$$J_2 = 1.0827 \times 10^{-3}$$

$$n_0 = \sqrt{\mu/a^3} \quad (\text{mean motion})$$

$$\mu = 3.986012 \times 10^{14} \text{ m}^3/\text{s}^2 \quad (\text{gravitational constant})$$

$\dot{\Omega}$, computed in MKS units, comes out in units of radians/second. It is more useful to convert it to degrees/day which is done by multiplying it by the conversion factor

$$\frac{180^\circ}{\pi \text{ radians}^*} \quad 86400 \text{ sec/day} = 4950355.3 \quad .$$

In equation (B-1), the quantity Ω_0 , the right ascension of the ascending node at orbital insertion, is given by

$$\Omega_0 = \lambda_0 + \text{GST} \sim \lambda_0 + [\text{GST}_{\text{MNO}} + \dot{L} * \text{DOY} + \omega_e * \text{GMT}] \quad (\text{B-3})$$

where

λ_0 = longitude of the ascending node at orbital insertion which is a function of orbital inclination, altitude and launch profile.

GST = Greenwich siderial time or the hour angle of the vernal equinox measured from the Greenwich meridian.

GST_{MNO} = GST at midnight on January 1 of any given year ($\approx 100^\circ$).

ω_e = rotational rate of Earth ($15^\circ/\text{hr}$).

GMT = Greenwich Mean Time of Day at orbital insertion
 = GMT_{Launch} + MET_{Insertion} .

The only quantity listed above that is not readily available from standard references is λ_0 .

λ_0 can be calculated approximately from spherical trigonometry as illustrated in Figure B-1 and some assumptions on the launch profile. From Figure B-1, one can see that if orbital insertion occurred at the launch site the longitude of the ascending node would be given by

$$\sin (\lambda_N - \lambda_{\text{LS}}) = \cot i \tan \delta_{\text{LS}}$$

or

$$\lambda_N = \lambda_{\text{LS}} + \sin^{-1} \left[\frac{\tan \delta_{\text{LS}}}{\tan i} \right]$$

where λ_{LS} is the longitude of the launch site ($-80.^\circ 6$) and δ_{LS} is the latitude of the launch site ($28.^\circ 5$). Both terms on the right side of the above equation for λ_N are to be taken as negative (west of Greenwich). Insertion, however, does not occur at the launch site but at a downrange position in the orbit plane, $\Delta u / \dot{u} * \omega_e$, added to it so that finally,

$$\lambda_0 = - \left[\lambda_{LS} + \sin^{-1} \left[\frac{\tan \delta_{LS}}{\tan i} \right] + \left[\frac{\Delta u}{\dot{u}} \right] * \omega_e \right] \quad (B-4)$$

Δu varies with altitude, inclination, and launch profile, $\dot{u} \approx 240^\circ/\text{hr}$ and $\omega_e = 15^\circ/\text{hr}$.

On one of the early iterations of the SPACELAB 1, as an example, we had

$$\begin{aligned} i &= 57^\circ & LD &= 12/3/80 & DAY &= 337 \\ \delta_{LS} &= 28.^\circ 5 & LT &= 18:00 \text{ GMT} \\ \lambda_{LS} &= 80.^\circ 6 & INS \text{ Time} &= 0.716 \text{ hr} \\ u_{iNS} &= 188.^\circ 77 & u_0 &= \sin^{-1} \left[\frac{\sin \delta_{LS}}{\sin i} \right] = 34.^\circ 67 \\ \Delta u &= u_{iNS} - u_0 = 154.^\circ 2 \end{aligned}$$

$$\lambda_0 \approx - \left[80.^\circ 6 + 20.^\circ 65 + \frac{154.^\circ 2}{240} \cdot 15 \right] = -110.^\circ 9$$

$$GST \approx [100^\circ + 0.9856 \cdot 337 + 15 \cdot 18.716] = 352.^\circ 9$$

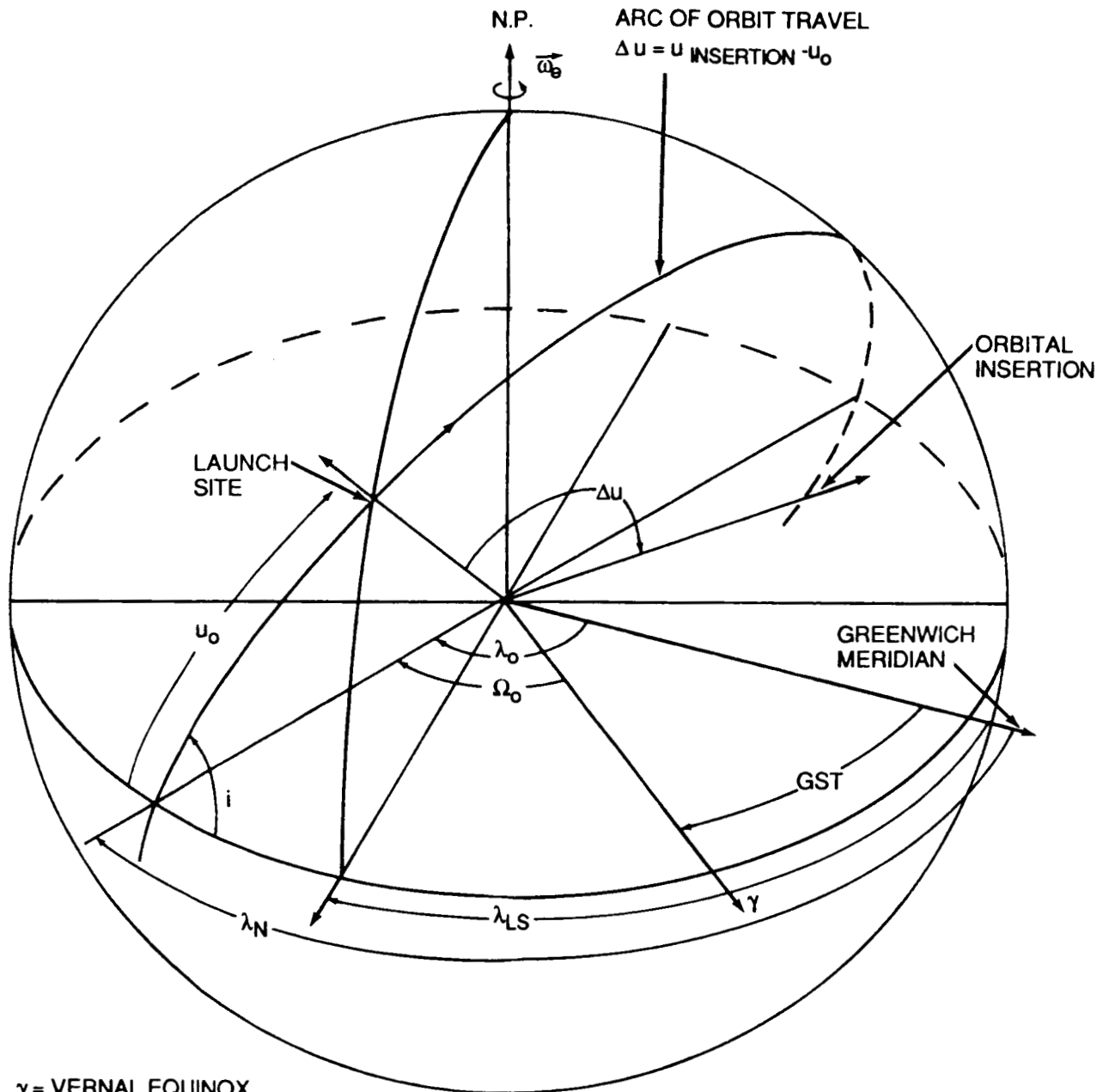
$$\Omega_0 \approx \lambda_0 + GST = 352.^\circ 9 - 110.^\circ 9 = 242.^\circ 0$$

The actual value of Ω_0 was $242.^\circ 685$.

The largest contributing error to λ_0 will be due to the uncertainty Δu in the downrange insertion distance from the launch site. This term is multiplied by the factor $15/240 = 0.0625$ however, so even a 10° error in the downrange position will contribute an error of only $0.^\circ 6$ in the position of the node which will not be significant for feasibility calculations.

Based on several previous flights, a downrange insertion value of $\Delta u = 155^\circ$ seems to be a good average value although, on occasion, a flight may have a value of 15° or 20° more than this, depending on the trajectory shaping.

For the very specific case of the ASTRO-1 mission with $i = 28.^\circ 5$ and $\text{alt} \approx 350$ km, we show in Figure B-2 the right ascension of the ascending node at orbital insertion for any given launch time of day for a launch on the first day of the month for any month of the year. With a little interpolation one can use this chart to get a very good value for Ω for any day of the year.



γ = VERNAL EQUINOX
 λ_{LS} = LONGITUDE OF LAUNCH SITE
 λ_N = LONGITUDE OF ASCENDING NODE OF ORBIT PLANE
 Ω_0 = RIGHT ASCENSION OF ASCENDING NODE OF ORBIT PLANE

Figure B-1. Illustration of the ascending node of the orbit plane relative to the meridian of Greenwich, England and to the vernal equinox.

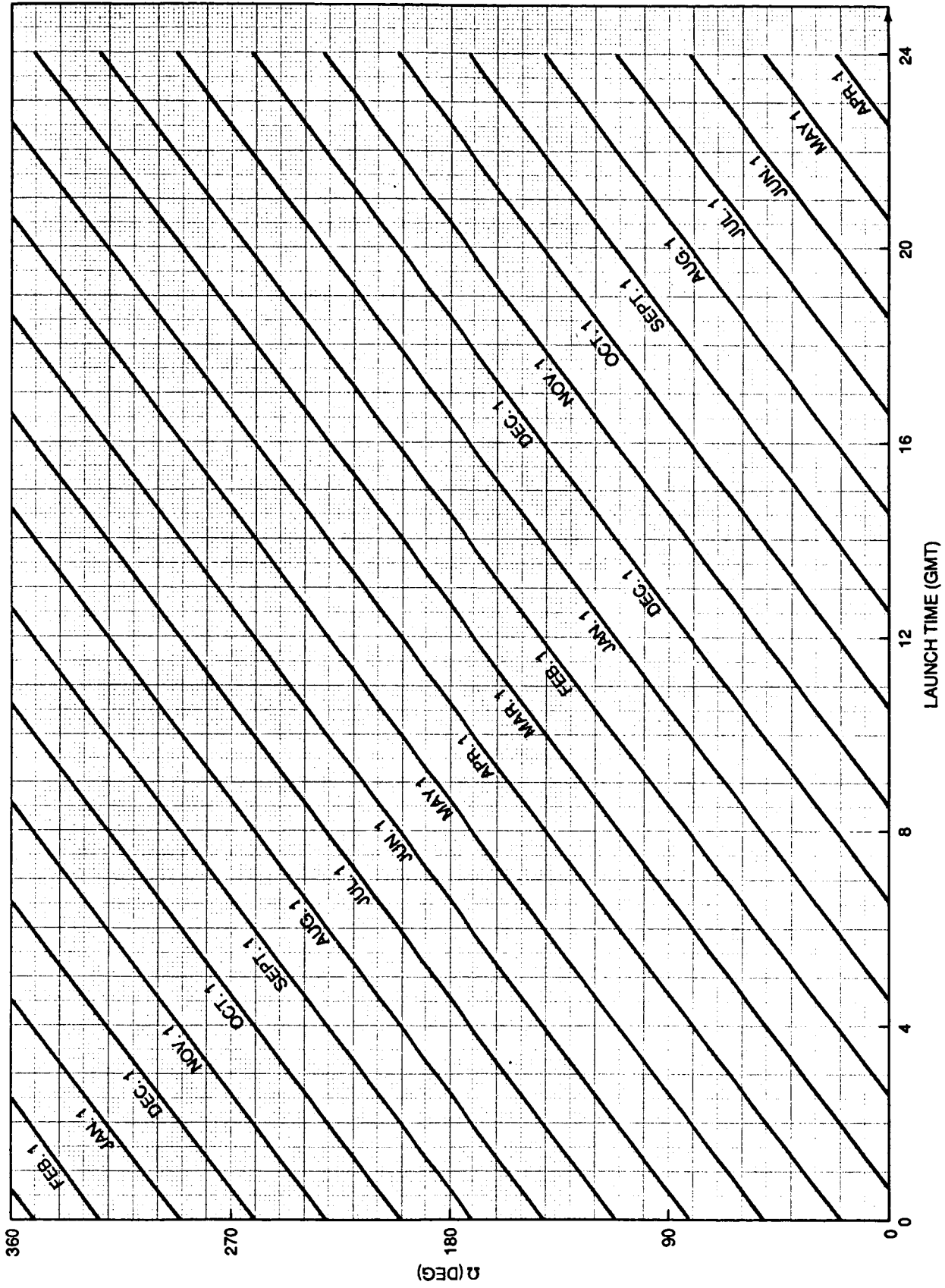


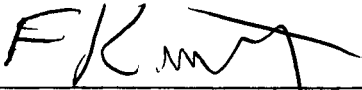
Figure B-2. Right ascension of the ascending node of the orbit plane as a function of launch date and launch time for ASTRO orbits ($i = 28.^\circ 5$, Alt = 350 km).

APPROVAL

CELESTIAL TARGET OBSERVABILITY FOR
ASTRO SPACELAB MISSIONS

By Larry D. Mullins

The information in this report has been reviewed for technical content. Review of any information concerning Department of Defense or nuclear energy activities or programs has been made by the MSFC Security Classification Officer. This report, in its entirety, has been determined to be unclassified.



G. D. HOPSON
Director, Systems Analysis and
Integration Laboratory



1. REPORT NO. NASA TM - 86591		2. GOVERNMENT ACCESSION NO.		3. RECIPIENT'S CATALOG NO.	
4. TITLE AND SUBTITLE Celestial Target Observability for Astro Spacelab Missions				5. REPORT DATE March 1987	
				6. PERFORMING ORGANIZATION CODE	
7. AUTHOR(S) Larry D. Mullins				8. PERFORMING ORGANIZATION REPORT #	
9. PERFORMING ORGANIZATION NAME AND ADDRESS George C. Marshall Space Flight Center Marshall Space Flight Center, Alabama 35812				10. WORK UNIT NO.	
				11. CONTRACT OR GRANT NO.	
				13. TYPE OF REPORT & PERIOD COVERED Technical Memorandum	
12. SPONSORING AGENCY NAME AND ADDRESS National Aeronautics and Space Administration Washington, D.C. 20546				14. SPONSORING AGENCY CODE	
15. SUPPLEMENTARY NOTES Prepared by Systems Analysis and Integration Laboratory, Science and Engineering Directorate.					
16. ABSTRACT <p>This report presents the mathematical technique for calculating the amount of time that an astronomical object, e.g., a star, can be observed from a satellite in a near Earth orbit. This includes the places and times in the orbit where the object is acquired and where it is lost. Constraints placed on the observation of the object, such as the line-of-sight from observer to the target must not come within less than some specified angle to the limb of the Earth, are included in the calculations.</p> <p>The equations developed within the report are then used for a detailed analysis of the observation possibilities for objects at any place on the celestial sphere for a typical Spacelab ASTRO mission. The results, presented in graphic form, are suitable for use in pre-mission planning and also for use in real-time replanning.</p>					
17. KEY WORDS ASTRO Spacelab Missions Celestial Target Observability Mission Planning Real Time Replanning			18. DISTRIBUTION STATEMENT Unclassified - Unlimited		
19. SECURITY CLASSIF. (of this report) Unclassified		20. SECURITY CLASSIF. (of this page) Unclassified		21. NO. OF PAGES 58	22. PRICE NTIS